Supplement to "The Atmospheric Chemistry and Climate Model Intercomparison Project (ACCMIP): Overview and description of models, simulations and climate diagnostics" by J.-F. Lamarque et al.

This supplement contains

(1) Description of all 16 models in ACCMIP, alphabetically listed
(2) Figures
(3) Tables

The description of each model contains additional information to what is available in the main portion of the paper. It is designed to cover all aspects relavant to chemistry modeling.

The figures displayed pertain to the physical climate variables discussed in the paper, namely temperature, specific humidity, precipitation and zonal wind. In particular, the performance of each model is shown whenever available. We have also included a version of Figures 8 and 9 in which a consistent set of models is used in all timeslices.

Tables list the requested output (also known as CMOR tables) in ACCMIP. These are also available at http://www.giss.nasa.gov/projects/accmip/tables.html.

1. CESM-CAM-Superfast

The CESM atmospheric chemistry-climate model used for CMIP5 was primarily developed at the U.S. National Center for Atmospheric Research and Lawrence Livermore National Laboratory, and is based on the Community Climate System Model version 4 (CCSM4; Gent, et al., 2011). We used the CCSM4 configuration with fully interactive land surface and terrestrial carbon cycle, but specified sea-surface and sea-ice properties from various CMIP5 simulations(except for the RCP2 & 6 simulations that inadvertently used temperatures from an earlier version, CCSM3). The implementation of the processes that involve interaction between chemical tracers and the physical atmosphere (such as wet deposition and convection) is described in Lamarque et al. (2012). The chemistry mechanism is a simplified version of the LLNL-IMPACT chemistry scheme (Rotman et al., 2004) to simulate the main free troposphere processes relevant to climate change, as described in a Cameron-Smith et al. (2006), but updated to use the rate constants specified in JPL Publication 06-2, with addition of a single isoprene tracer, and omitting the species that are only relevant to the stratosphere. Stratospheric ozone is simulated instead using Linoz version 2 (Hsu and Prather, 2009), with an additional simple loss to simulate polar ozone holes using the method of Cariolle, et al, 1990, with parameters calculated for each decade. The whole chemical mechanism uses 15 tracers. The 3D methane distribution was specified using the output of simulations of an earlier model (CAM3.5) that used a more complete chemical mechanism (from NCAR-CAM3.5). The chemical emissions for the historical and RCP simulations followed Lamarque et al (2010 for historical, 2011 for RCPs). This version of our model fixed the error in some previous versions that resulted in zero NOx from lightning, as well as a typographical error in the rate constant for CO + OH -> CO2 + HO2 (except for our RCP2 and RCP6 simulations) that previously resulted in excessive carbon monoxide concentrations that almost exactly compensated to give the correct rate for the reaction (so the error had little effect on the rest of the simulation). Caution should also be used when cross comparing the RCP2 & 6 simulations to the other scenarios because the ocean temperatures were inadvertently derived from a different model version (CCSM3 instead of CCSM4).

2. CICERO-Oslo-CTM2

OsloCTM2 is an off-line atmospheric chemistry transport model, driven by meteorological data generated by the Integrated Forecast System (IFS) model at the European Centre for Medium-Range Weather Forecasts (ECMWF). It is possible to run the model with different resolutions. In these simulations the resolution used is T42, with 60 vertical layers ranging up to 0.1 hPa. The tropospheric chemistry scheme (Berntsen and Isaksen, 1997; Skeie et al., 2011b) and the modules for sulphate, nitrate, black carbon (BC), primary organic carbon (OC), secondary organic aerosols (SOA), mineral dust and sea salt are used. The stratospheric chemistry scheme is not included in the ACCMIP simulations.

Time slice simulations is performed, and each simulation is one year long and meteorological data for year 2006 are used in all simulations. Each simulation is initialized by the same pre-industrial model climatology and a three year spin up is used. The historical simulations are described in Skeie et al. (2011b).

The tropospheric chemistry scheme includes 51 species, 86 thermal reactions, 17 photolytic reactions, 2 heterogeneous reactions. Photo dissociation rates are calculated on-line once every model hour, and reaction rates are from JPL Jet Propulsion Laboratory of National Aeronautics and Space Administration. The photo dissociation rates account for scattering and absorption by clouds, aerosols and molecules, however the modelled aerosols are not yet coupled with the dissociation rates in the Oslo CTM2. The numerical integration of chemical kinetics is done applying the Quasi Steady State Approximation (QSSA) (Hesstvedt *et al.*, 1978). In the stratosphere monthly model climatological values of ozone and nitrogen species are used, except in the 3 lowermost layers in the stratosphere (approximately 2.5 km) where the tropospheric chemistry scheme is applied to account for photochemical O_3 production in the lower stratosphere due to emissions of NOx, CO and VOCs.

The sulphur chemistry scheme is coupled with the oxidant chemistry (Berglen et al., 2004). A simple bulk scheme is used for BC and OC with aging times dependent on season and latitude (Skeie et al., 2011a). The scheme for SOA are described in Hoyle et al. (2007). We allow the semi-volatile species to partition to ammonium sulphate aerosols as well as existing organic aerosols. For nitrate, a thermodynamical model is used where chemical equilibrium between inorganic compounds is simulated, including sea salt. The nitrate module is described in Myhre et al. (2006) and the sea salt module in Grini et al. (2002). The mineral dust emissions are driven by wind (Grini et al., 2005), and no changes in the dust emissions are assumed for the historical time period. In total 137 components are treated in the model.

The natural emissions are assumed to be constant throughout the simulation period. The lightning emissions are based on Price et al. (1997) scaled to 5 Tg N $year^{-1}$ and distributed over the year by convection activity data. The natural emissions of CO, NOx, and hydrocarbons from vegetation, ocean and soil are from the POET emission inventories (Granier et al., 2005). The isoprene and biogenic volatile organic compounds (VOCs) important in SOA formation are as used in Hoyle et al. (2009). The isoprene emissions are 220 Tg $year^{-1}$.The natural emissions of sulphur species are as described in Berglen et al. (2004) except that the parameterizations of the DMS flux from Nightingale et al. (2000) and emission from continuous degassing volcanoes from Dentener et al. (2006) are used. The total natural emissions are presented in Table 1 in Skeie et al. (2011b).

Advection of tracers is calculated using the second order moment scheme (Prather, 1986). Vertical transport by convection is based on mass flux data from IFS (Tiedtke, 1989) and an "elevator" principle, surplus or deficit of mass in a column as described in Berglen et al. (2004). Turbulent mixing in the boundary layer, is parameterized according to the Holtslag K-profile scheme (Holtslag et al., 1990).

The dry deposition velocity for each component is dependent on season and surface type. Wet deposition is divided into large scale systems and convective events. The wet deposition is calculated based on meteorological data for convective activity, cloud fraction and rainout and the solubility of the species. Soluble components are removed proportionally to the fraction of the clouds which rains out. For partly soluble components, Henry's law is used to calculate the fraction of components inside the cloud that is dissolved in cloud water. The aerosol optical properties are calculated with Mie Theory and information of size distribution and refractive indexes are given in Myhre et al. (2007). The radiative transfer calculations are performed with the discrete ordinate method (Stamnes et al., 1988) with 4 spectral regions and 8-streams (Myhre et al., 2009).

3. CMAM

The Canadian Middle Atmosphere Model is based on a vertically extended version of the third-generation Canadian GCM (CGCM3.1) described in Scinocca et al. (2008). The gas-phase chemical mechanism is tailored for the stratosphere, including the major O_x, HO_x, NO_x, Cl_y and Br_y reactions of importance to the stratosphere, and comprised of 108 chemical reactions and 39 photolysis reactions (updated from Jonsson et al., 2004). For the troposphere, with available inorganic Cl and Br almost completely sequestered in reservoir species, the mechanism reduces to methane-NO_x chemistry. Clear-sky photolysis rates are interpolated from a pre-calculated look-up table. The clear-sky rates are corrected to account for clouds using the instantaneous model cloud field following the method of Chang et al. (1987), modified to account for attenuation of cloud effects on photolysis rates above the clouds.

Heterogeneous chemistry in the troposphere accounts for N_2O_5 hydrolysis on a specified monthly-average background aerosol. In the stratosphere, hydrolysis of N_2O_5 and $BrONO_2$ is calculated on specified monthly zonal mean SAD fields (SPARC, 2006) with a repeating annual cycle constructed from the data for the year 2000 used for all years. Heterogeneous chemistry additionally accounts for six reactions each on type Ib and II PSCs using a prognostic calculation of PSC occurrence based on local thermodynamic conditions (Carslaw et al., 1995). Dry deposition is based on a multiple resistance methodology using the instantaneous surface parameters from the GCM land surface scheme while wet deposition includes solubility based removal of species from stratiform precipitation (Giorgi and Chameides, 1986) and deep convective updrafts, in addition to below-cloud washout of HNO_3 and H_2O_2.

The model carries 42 chemical species and these are grouped together in families, where applicable, yielding a total of 25 advected species. Transport of the chemical species is calculated with spectral advection in the horizontal and a finite element scheme in the vertical. To control the appearance of Gibbs phenomenon due to the use of spectral advection for fields with sharp gradients a ‘physics filter’ is employed whereby the fields passed to the package of physical parameterizations (including chemistry) is spectrally filtered before entering the physics and the tendencies returned from the physics are similarly filtered before being added to the model variables (Lander and Hoskins, 1997). The use of a physics filter helps to ameliorate some of the most trouble-some aspects of spectral advection, though for very short-lived species (the NOx family and HNO_3) a non-linear function of the physical values of the tracer field is taken before the field is transformed to spectral space. The process is referred to as ‘hybridization’ and is a generalized version of a similar approach used in earlier versions of the Canadian GCM for the advection of water vapour. A more detailed description of hybridization and an example of the use of hybridization for Radon-222 is given in Scinocca et al. (2008).

Pre-industrial emissions of NO_x from soils were constructed by taking the annually repeating monthly fields from the RETRO project (Schultz et al., 2007) for present-day conditions (30.7 Tg-NO_2/year) and subtracting the anthropogenic component of soil NOx emissions given for the year 2000 (2.13 Tg-NO_2/year) in the CMIP5 database (Lamarque et al., 2010). Soil NO_x emissions for a particular year are then given by adding the appropriate CMIP5-specified anthropogenic component to the constructed pre-industrial field. Combining the RETRO and CMIP5 emission fields are performed using gridded annual total emissions; the annual cycle from the original RETRO emissions is then applied to generate monthly fields.

Emissions of NO_x from lightning are constructed using a parameterization based on the updraft mass flux calculated by the model deep convection parameterization (Zhang and

McFarlane, 1995) following the approach of Allen and Pickering (2002). Cloud-to-ground flashes are assumed to yield two times as much NO_x as cloud-to-cloud flashes (360 and 180 moles/flash) giving a total of approximately 13 Tg-NO_2/year for present-day conditions. Note that the convective updraft mass flux is taken from the model level closest to, but above, 400 hPa so the temporal evolution of lightning will depend on the evolution of the convective mass flux at a particular pressure level. Further research is required to understand the climate change effects on the model parameterized lightning NO_x emissions, in particular the use of the updraft mass flux at a constant pressure level.

For the ACCMIP runs the model has been run at T47 spectral resolution with 71 vertical levels and a model lid at approximately 95 km. All timeslice experiments were run for 20 years, discarding the first ten years as spinup. A repeating annual cycle of SSTs and sea-ice was constructed for each timeslice by averaging 11 years of output from two ensemble members from the CCCma coupled model (CanESM2) runs submitted to CMIP5.

4. EMAC

The ECHAM/MESSy Atmospheric Chemistry (EMAC) model is a numerical chemistry and climate simulation system that includes submodels describing tropospheric and middle atmosphere processes and their interaction with oceans, land and human influences (Jöckel et al., 2006). It uses the Modular Earth Submodel System (MESSy) to link multi-institutional computer codes. The core atmospheric model is the 5th generation European Centre Hamburg general circulation model (ECHAM5, Roeckner et al., 2006). For the present study EMAC (ECHAM 5.3.01/MESSy 1.10) is applied in the T42L90MA-resolution, i.e. with a spherical truncation of T42 (corresponding to a quadratic Gaussian grid of approximately 2.8°×2.8° degrees in latitude and longitude) with 90 vertical hybrid pressure levels up to 0.01 hPa.

Gas-phase chemistry is calculated with the submodel MECCA (Sander et al., 2005), which deals with both tropospheric and stratospheric chemistry. The chemical mechanism is integrated in the entire model domain, i.e., consistently from the surface to the stratosphere. It is important to highlight that no arbitrary or artificial "intermediate boundary conditions" (for instance at the tropopause or between layers) are prescribed. This means that in particular the stratosphere-to-troposphere transport of ozone is simulated self-consistently, i.e., with a single ozone tracer. Chemical species are advected according to the algorithm of Lin and Rood (1996), which is part of ECHAM5. For the present study, the EVAL chemical mechanism (Jöckel et al., 2006) is adopted, consisting of 179 gas phase reactions (including ozone tropospheric chemistry, non-methane hydrocarbons up to isoprene and stratospheric chemistry for bromine and chlorine), 61 photolysis reactions and 10 PSC reactions. Additional heterogeneous, acid-base and aqueous-phase reactions are included in the submodel SCAV (Tost et al., 2006a). Reaction rates for heterogeneous and photolysis reactions are computed by the submodels HETCHEM and JVAL, respectively.

The convection processes (submodel CONVECT, Tost et al. 2006b) are simulated following the Tiedtke (1989) scheme with the Nordeng (1994) closure, as in ECHAM5 (Roeckner et al., 2006). Convective tracer transport is realized in the CVTRANS submodel (Jöckel et al., 2006) using the bulk approach. Cloud related quantities are calculated by the CLOUD submodel, following the original ECHAM5 routine by Lohmann and Roeckner (1996). Polar stratospheric clouds are modelled by the PSC submodule (Kirner et al., 2011). Dry and wet deposition are handled by the submodels DRYDEP and SEDI (Kerkweg et al., 2006a) and by SCAV (Tost et al., 2006a), respectively.

The radiation calculations take into account prognostic cloud cover, cloud water, cloud ice (from the CLOUD submodel) and prognostic specific humidity. Forcings from radiatively active gases (CO_2, CH_4, O_3, N_2O, $CFCl_3$ (CFC-11) and CF_2Cl_2 (CFC-12)) are computed from the corresponding prognostic tracers within the RAD4ALL submodel. Since the ACCMIP model simulations are run without a detailed aerosol module, the standard ECHAM5 aerosol climatology (Tanre et al., 1984) is used to drive radiation calculations.

The time-slices are run with prescribed SSTs/SICs (10 year climatological mean around the base year). Monthly mean SSTs and SICs are prescribed from the CMIP5 run carried out with the CMCC Climate Model. The SSTs/SICs on the ORCA coordinates are interpolated to a T42 grid using the ECHAM land masking. The CMCC climate model is based on the same ECHAM5 atmospheric component as EMAC, although it uses a T63L95 resolution and a different shortwave radiation scheme (see Cagnazzo et al., 2007 for a description).

Offline and online emissions are supplied to the model via the OFFLEM and ONLEM submodels (Kerkweg et al., 2006b), respectively. In the current setup, emissions of NO, CO, SO_2, NH_3 and VOCs (C_2H_4, C_2H_6, C_3H_6, C_3H_8, C_4H_{10}, CH_3CHO, CH_3COCH_3, CH_3COOH, CH_3OH, HCHO, HCOOH and methyl-ethyl-ketone (MEK)) are considered. Anthropogenic and biomass burning emissions are provided offline and are taken from Lamarque et al.

(2010) in the past and from the corresponding RCP scenarios in the future. Natural emissions include isoprene and soil NO, lightning NO_x (calculated online by the LNOX submodel, using the Grewe et al., 2001 scheme), while biogenic CO and other VOCs (C_2H_4, C_2H_6, C_3H_6, C_3H_8, C_4H_{10}, CH_3COCH_3, CH_3COOH, CH_3OH and HCOOH, Ganzeveld et al., 2006), volcanic SO_2 (Dentener et al., 2006) and terrestrial DMS (Spiro et al., 1992) are provided as offline fields. Boundary condition data for long-lived species (CO_2, N_2O, CH_4, CFCs, HCFCs and halons) are included by means of the TNUDGE submodel, using data from Prinn et al. (2000) for the 2000 simulation and rescaled to the corresponding year/scenario for the other experiments, using concentration data from Meinshausen et al. (2011).

The additional submodels adpopted for these experiments include: AIRSEA (tracer exchange between atmosphere and ocean, Pozzer et al., 2006), DRADON (diagnostic of tracer transport using 222-Rn decay), PTRAC and TRACER (prognostic tracers, Jöckel et al., 2008) and TROPOP (tropopause diagnostics).

The 2000 simulation has been evaluated in quite some detail as part of a Master thesis (see simulation EMAC-ACCMIP in http://www.pa.op.dlr.de/~VeronikaEyring/Publications/2011_Klinger_Masterthesis_FINAL.pdf). A corresponding publication (Klinger et al., in prep.) will be shortly submitted to GMD and, together with Jöckel et al. (2006), may serve as a reference for EMAC.

5. GEOSSCM

The GEOS Chemistry Climate Model (GEOSCCM), described in *Oman et al.* [2011], couples the Global Modeling Initiative (GMI) stratospheric and tropospheric chemistry mechanism [*Duncan et al.*, 2007; *Strahan et al.*, 2007] to the Goddard Earth Observing System (GEOS) version 5 general circulation model [*Rienecker et al.*, 2008; *Molod et al.*, 2012]. The GEOS5 AGCM uses a finite volume dynamical core [*Lin*, 2004] and the Relaxed Arkawa-Schubert scheme [*Moorthi and Suarez*, 1992] for convection. It includes 72 vertical levels extending from 0.01 hPa to the surface. The horizontal resolution of the GEOSCCM for the ACCMIP simulations is 2 degrees latitude by 2.5 degrees longitude.

The GMI chemical mechanism has 117 species and includes 321 thermal reactions and 81 photolysis reactions. The troposphere includes detailed O_3-NO_x-hydrocarbon chemistry [*Bey et al.*, 2001] with updates by *Duncan et al.* [2007]. Photolysis rates are calculated using Fast-JX [*Wild et al.*, 2000; *Bian and Prather*, 2002] with updates. Isoprene and other biogenic VOC emissions are calculated within the model based on the MEGAN emission model [*Guenther et al.*, 1999]. Temperature and precipitation-dependent soil NO_x emissions based on *Yienger and Levy* [1995] are also calculated online. Lightning NO_x emissions are from a monthly climatology based on *Price et al.* [1997] and scaled to 5 TgN/year. GEOSCCM includes both wet and dry deposition. The dry deposition method, described in *Wang et al.* [1998], is based on resistance-in-series. The ACCMIP simulations use monthly mean offline aerosol fields for black and organic carbon, sulfate, sea salt, and dust. Stratospheric sulfate surface area density is based on satellite observations and is constant for all years.

The GEOSCCM ACCMIP simulations are conducted as “time slices”, in which SSTs vary year-to-year while trace gas emissions, greenhouse gases, and ozone depleting substances remain fixed within each timeslice. Following spin-up, we conduct at least 10 years of simulation for each timeslice. The historic simulations for 2000 and 1980 are driven by observed SSTs from *Reynolds et al.* [2002]. The 1850 simulation uses 1870s AMIP SSTs (http://www-pcmdi.llnl.gov/projects/amip/AMIP2EXPDSN/BCS/bcsintro.php), which are based on HadISST v1 and NOAA OI SST v2 [Hurrell et al. (2008)]. SSTs for the RCP6.0 2100 simulation come from the RCP 6.0 simulation of the CCSM4 [*Meehl et al.*, 2012].

6. GFDL-AM3

GFDL-AM3 is the atmospheric component of the GFDL coupled ocean-atmosphere-land-ice model (CM3) (Donner et al., 2011; Griffies et al., 2011). It simulates tropospheric and stratospheric chemistry interactively over the full model domain (Austin et al., submitted; Naik et al., submitted). The model uses a finite-volume dynamical core on a horizontal domain consisting of 6x48x48 cubed-sphere grid (Putman and Lin 2007) with the grid size varying from 163 km (at the 6 corners of the cubed sphere) to 231 km (near the center of each face), a resolution denoted as C48. The vertical domain of the model extends from the surface up to 0.01 hPa (86 km) with 48 vertical hybrid sigma pressure levels. AM3 simulates atmospheric distributions of 97 chemical species (81 gas, 16 aerosol) that undergo 41 photolytic, 182 gas phase, and 13 heterogeneous reactions (4 tropospheric and 9 stratospheric) throughout the model domain. Reaction rates are from Sander et al. (2006). Tropospheric trace gas chemistry in AM3 includes reactions of NO_x-HO_x-O_x-CO-CH_4 and NMVOCs based on the chemical scheme used in the Model for OZone and Related Tracers version 2 (MOZART-2) (Horowitz et al., 2003) with updates in the isoprene nitrate chemistry (Horowitz et al, 2007). AM3 simulates the mass distribution of aerosols (SO_4, BC, OA, NO_3, dust and sea-salt) based on their emissions, chemical production and processing, transport, and depositional losses. The chemical production of sulfate aerosols from SO_2 and dimethyl sulfide is fully coupled with the gas-phase chemistry. Stratospheric chemistry in AM3, based on the formulation of Austin and Wilson (2010), includes the stratospheric O_3 loss cycles (O_x, HO_x, NO_x, ClO_x, and BrO_x), and heterogeneous reactions on liquid ternary solutions and ice and nitric acid trihydrate (NAT) polar stratospheric clouds. Heterogeneous reactions on liquid ternary solutions are represented based on Carslaw et al. (1994) and those on NAT polar stratospheric clouds are calculated as in Hanson and Mauresberger (1988). As discussed in Donner et al. (2011), the rates of change of inorganic chlorine (Cly) and inorganic bromine (Bry) are parameterized as a function of tropospheric concentrations of source gases (CFC11, CFC12, CH_3Cl, CCl_4, CH_3CCl_3, and HCFC22 for Cl_y, and CH_3Br, Halon1211 and Halon1301 for Br_y), to minimize computational cost. Changes in tropospheric and stratospheric ozone, water vapor, and all aerosols, except NO_3, feedback to atmospheric radiation calculations.

Dry deposition velocities of gaseous species other than O_3 and PAN are calculated offline using a resistance-in-series scheme as described by Horowitz et al. (2003). Dry deposition velocities for O_3 are taken from Bey et al. (2001) and those for PAN are from a simulation of MOZART-4 calculated interactively to reflect the updates described by Emmons et al. (2010). Dry deposition of aerosols includes gravitational settling and turbulent impaction at the surface. Wet deposition of soluble gaseous and aerosol species includes in-cloud and below-cloud scavenging by large-scale (ls) and convective clouds (cv) and are simulated as first-order loss processes (Donner et al., 2011; Fang et al., 2011; Naik et al., submitted). A multivariate interpolation table from calculations using the Tropospheric Ultraviolet and Visible radiation model version 4.4 (Madronich and Flocke, 1998) is used to compute clear-sky photolysis frequencies as a function of pressure, solar zenith angle, surface albedo, temperature, and simulated overhead ozone column, which are then adjusted for clouds, but do not account for simulated aerosols.

Anthropogenic (including shipping and aircraft) and biomass burning emissions are from the inventories of Lamarque et al. (2010) and Lamarque et al. (2011) for historical and future scenarios, respectively. Natural emissions for CO, ethene, ethane, propene, propane, acetone, methanol, ethanol, isoprene, and terpenes are from the POET inventory (Precursors of Ozone and their Effects in the Troposphere) for 2000 (Granier et al., 2005) as implemented in MOZART-4 (Emmons et al. 2010). Natural soil NO_x emissions are set to preindustrial value of 3.6 Tg N yr^{-1} as in Horowitz (2006) for all ACCMIP simulations. Lightning NO_x emissions

in the model are calculated interactively following Horowitz et al. (2003) as a function of subgrid convection parameterized in AM3 (Donner et al., 2011) with annual totals ranging from 3-6 Tg N yr^{-1}.

For the ACCMIP simulations, AM3 is driven by 10-year climatological monthly mean sea surface temperature and sea-ice cover taken from the corresponding (historical or RCP) simulations of CM3 conducted according to the CMIP5 specifications in support of the IPCC-AR5 (John et al., 2012; Horowitz et al. in preparation). Each simulation is conducted for 11 years with the first year used as spin up. Globally uniform concentrations of CO_2, CH_4, N_2O, and halocarbons (CFC-11, CFC-12, CFC-113, CCl_4, CH_3Cl, CH_3CCl_3, HCFC-22, Cl_y, and Br_y) are prescribed from the Representative Concentration Pathways database (Meinshausen et al., 2011). Global mean concentrations of CH_4 and N_2O are specified at the surface as lower boundary conditions for chemistry. No volcanic stratospheric aerosols were considered for all ACCMIP simulations and a static vegetation distribution for the corresponding simulation year (taken from CM3 simulations) was used for the land component of the model.

7. GISS-E2-R

The GISS-E2-R model was run at 2° latitude by 2.5° longitude resolution, with increased effective resolution for tracers by carrying higher-order moments at each grid box. The configuration used had 40 vertical hybrid sigma layers from the surface to 0.1 hPa (80 km). ACCMIP diagnostics for GISS-E2-R were saved from the GISS-E2-R CMIP5 transient climate simulations as those included fully interactive chemistry and aerosols. Those simulations were spun up for more than 1000 years, after which an ensemble of five simulations was performed for 1850-2005. Starting in 2006, simulations were branched into the 4 RCPs and extended through 2100. Additional simulations (e.g. Em2000Cl1850) were run for 40 years following a 10 year spinup, as was a companion Em1850Cl1850 that was used for comparison with Em2000Cl1850 to remove any difference in experimental setup as the EmXXXXClYYYY had fixed SSTs and sea-ice from the prior GISS-E2-R transient runs.

Dry deposition is calculated using a resistance-in-series model [Wesely and Hicks, 1977] coupled to a global, seasonally varying vegetation dataset. Wet deposition depends upon transport within convective plumes, scavenging within and below updrafts, rainout within both convective and large-scale clouds, washout below precipitating regions, evaporation of falling precipitation, and both detrainment and evaporation from convective plumes (Koch et al., 1999; Shindell et al., 2001)

The gas phase chemistry scheme included both tropospheric and stratospheric chemistry, with 156 chemical reactions among 51 species. Five of these reactions are heterogeneous, taking place on either/or polar stratospheric clouds, sulfate or dust aerosols. The model includes sulfate, nitrate, carbonaceous (black and organic, both primary and secondary for the latter), mineral dust and sea-salt. Photolysis rates for 28 reactions are calculated, 26 of which use the Fast-J2 scheme [Bian and Prather, 2002] with two additional reactions important only at very high altitudes parameterized. Note that the model includes a reaction pathway for HO2 + NO to yield HNO3 [Butkovskaya et al., 2007].

Natural emissions in 2000 are NOx from lightning (7.3 Tg N yr-1) and biogenic alkenes (16 Tg C yr-1), paraffins (14 Tg C yr-1), isoprene (536 Tg yr-1) and terpenes (192 Tg yr-1). These emissions all vary with climate [D T Shindell et al., 2006]. Natural emissions of NOx from soils are prescribed at fixed values (2.7 Tg N yr-1). Methane emissions from wetlands were not used prior to 2005 in GISS simulations as historical methane concentrations were prescribed, but methane concentrations were calculated internally from emissions during 2006-2100. Present day model wetland emissions are 197 ± 4 Tg yr-1 in the first 5 years of the 4 transient simulations.

Tracer transport uses a nondiffusive quadratic upstream scheme [Prather, 1986].

8. GISS-E2-R-TOMAS

The TwO-Moment Aerosol Sectional (TOMAS) aerosol microphysics model has been implemented into the climate model of GISS-ModelE that is referred as "GISS-E2-R-TOMAS" model (Lee and Shindell 2012, in preparation). The GISS-E2-R-TOMAS uses 2° latitude by 2.5° longitude resolution with 40 vertical hybrid sigma layers from the surface to 0.1 hPa (80 km). The ACCMIP core timeslice and Em2000Cl1850 simulations were driven by the corresponding decadal-average sea-surface temperatures and sea-ice coverages from the GISS-E2-R CMIP5 transient climate simulations and were ran for 10 year after 3 year spin-up. The GISS-E2-R-TOMAS model had 146 tracers. The TOMAS model alone has 108 size-resolved aerosol tracers plus three bulk aerosol-phase and five bulk gas-phase species. TOMAS predicts aerosol number and mass size distributions by computing total aerosol number (i.e., 0^{th} moment) and mass (i.e., 1^{st} moment) concentrations for each species (sulfate, sea-salt, internally mixed elemental carbon, externally mixed elemental carbon, hydrophilic organic matter, hydrophobic organic matter, mineral dust, aerosol-water) in 12-size bin ranging from 10 nm to 10 um in dry diameter. (Lee and Adams, 2011). Water uptake by sulfate, sea-salt, and hydrophilic organic matter is accounted for in the model. Tracer transport scheme is same as GISS-E2-R.

Apart from 5 gas-phase species in the TOMAS model, the gas phase chemistry in GISS-E2-R-TOMAS used 47 species (i.e., 51 species in GISS-E2-R minus 4 gas phase SOA precursor species) and included 152 chemical reactions to account for tropospheric and stratospheric chemistry, which includes 5 heterogeneous reactions, and 28 reactions to compute photolysis rates – 26 of them used the Fast-J2 scheme [Bian and Prather, 2002]. Note that the GISS-E2-R-TOMAS model also includes a reaction pathway for HO2 + NO to yield HNO3 [Butkovskaya et al., 2007]. This is identical to the gas modeling included in GISS-E2-R but the gas phase modeling in the GISS-E2-R-TOMAS model is less extensive than GISS-E2-R and here are key differences related to gas modeling between two models: In GISS-E2-R-TOMAS, 1) Photolysis rates are not affected by aerosols, 2) Simple SOA modeling is used, and 3) Nitrate chemistry (Bauer et al., 2007) is not included.

Deposition scheme is basically same as GISS-E2-R (Koch et al., 1999; Shindell et al., 2001) except that size-resolved deposition processes are used for aerosols (Lee and Adams, 2011). For example, the modified Köhler theory is applied for aerosol in-cloud scavenging, and a size-dependent gravitational settling of particles and a size-dependent resistance in the quasi-laminar sublayer are used. Primary sulfate is assumed to be 2.5 % of anthropogenic emission of SO2. Natural emissions for gas phase in the 2000 timeslice simulations are NOx from lightning (2.9 Tg N yr-1) and biogenic alkenes (16 Tg C yr-1), paraffins (14 Tg C yr-1), isoprene (534 Tg yr-1) and terpenes (193 Tg yr-1). Only isoprene emission varies with climate (Shindell et al., 2006). Natural emissions of NOx from soils are prescribed at fixed values (2.7 Tg N yr-1). Methane emissions from wetlands were not used.

9. HadGEM2

For ACCMIP, HadGEM2 is configured as HadGEM2-ES (Collins et al., 2011; Martin et al., 2011) but with coupling to the ocean deactivated and instead running with fixed SSTs. The atmospheric horizontal resolution is 1.875deg × 1.25deg (~140 km at mid latitudes) and the model has 38 vertical levels with a top of ~39 km. HadGEM2 uses a 30 minute timestep in general and 5 minute timestep in the chemistry.

Each experiment has a time-slice of 10 years with a 1 month spinup. This was considered sufficient as the initialization was taken from the CMIP5 transient run of the appropriate climate and thus very close to a spun up state at the start of the run.

The imposed sea surface temperatures were taken as a decadal mean from the HadGEM2 CMIP5 transient run for the appropriate time period (Jones et al, 2011).

HadGEM2 is based on MetUM and uses its core dynamical components. The large scale convection is based on the new dynamical core (Davies et al., 2005). It is a non-hydrostatic, fully compressible, deep atmosphere formulation using a terrain-following, height-based vertical coordinate. Convective transport is treated according to the mass-flux scheme of Gregory and Rowntree (1990). The scheme is applied to dry and moist (shallow, deep, mid-level) convection.

HadGEM2 uses CLASSIC (Bellouin et al., 2011) which is a mass based aerosol scheme with natural (dust, sea salt and SOA) and anthropogenic (sulphate, black and organic carbon from fossil fuels) and biomass burning.

HadGEM2 includes the UKCA (UK Chemistry and Aerosols) model which allows selecting between several chemistry schemes. For the standard ACCMIP experiments we used UKCA-StdTC (standard troposheric chemistry; O'Connor et al., in preparation). UKCA-StdTC includes 41 species 26 of which are tracers. The ozone attribution experiments applied UKCA-ExtTC (extended tropospheric chemistry; Folberth et al., in preparation) which increases the number of tracers to 63 and the total number of species to 85. Neither of the two models include stratospheric chemistry.

The tropospheric chemistry schemes used in ACCMIP make use of the simple pre-computed setup using the offline Cambridge 2D-photolysis model (Law and Pyle, 1993) which is based on the two-stream approach of Hough (1988). Photolysis rates are read by UKCA and interpolated in space and time at each model grid box (no variability with clouds and aerosols). UKCA-StdTC includes 26 photolysis reactions. This number increases to 45 for UKCA-ExtTC. In both cases some reactions make use of a scaled rather than a pre-computed photolysis rate (e.g., in case of organic hydroperoxides).

Dry deposition at the surface is simulated using the resistance-in-series approach (Wesely, 1989). The multiple resistances are calculated for nine surface types and are then combined to give a grid-box mean deposition velocity. UKCA applies the Giannakopoulos et al. (1998) wet removal scheme. Wet removal of any species is governed by its solubility and uses the Henry's Law formulation.

Soil-biogenic NO_x emissions are prescribed using the monthly distributions provided by GEIA (http://www.geiacenter.org/inventories/present.html), which are based on the global empirical model of soil-biogenic NOx emissions of Yienger and Levy (1995). NOX emissions from global lightning activity are parameterized based on the convective cloud top height following Price and Rind (1992, 1994), and are thus sensitive to the model climate.

UKCA-ExtTC includes an interactive biogenic emission scheme for isoprene, (mono-) terpenes, acetone and methanol that uses the process-based approach of Arneth et al.(2007) and includes the CO2 inhibition effect (Young et al, 2009). In HadGEM2 this scheme yields 493 TgC/yr of isoprene under present-day conditions (Pacifico et al., submitted). Under pre-

industrial and future (RCP8.5) climate conditions the interactive scheme produces 609 TgC/yr and 484 TgC/yr, respectively.

10. LMDZ-OR-INCA

The Interaction between Chemistry and Aerosol (INCA) model is used to simulate the distribution of aerosols and gaseous reactive species in the troposphere. INCA computes primary emissions, deposition and chemical equations with a time-step of 30 min. INCA is coupled online to the LMDz General Circulation Model (GCM) to account, with different degrees of complexity, for climate chemistry interactions. In the simulations described here, LMDz is coupled with the ORCHIDEE (Organizing Carbon and Hydrology in Dynamic Ecosystems) dynamic global vegetation model (Krinner et al., 2005) for soil/atmosphere exchanges of water and energy (Hourdin et al. 2006), but not for biogenic CO_2 or VOC fluxes. Together, these three models form the LMDz-OR-INCA model. Fundamentals for the gas phase chemistry are presented in Hauglustaine et al. (2004) and first results with the full tropospheric gaseous chemical scheme are gathered by Folberth et al. (2006). The oxidative tropospheric photochemistry is described through 85 chemical species and 264 chemical reactions, including non-methane hydrocarbon oxidation.

For aerosols, the INCA model simulates the distribution of anthropogenic aerosols such as sulfates, black carbon (BC), particulate organic matter (POM), as well as natural aerosols such as sea-salt and dust. The aerosol code keeps track of both the number and the mass of aerosols using a modal approach to treat the size distribution, which is described by a superposition of log-normal modes (Schulz et al., 1998, 2007). The residence time of tropospheric aerosols varies from a few hours near the surface to more than 20 days in the high troposphere. The heterogeneity of the aerosol sources and the processes that they undergo in the atmosphere, make their size distribution extremely large from several nanometers to a hundred microns for dust and sea-salt. To treat the aerosol size diversity, particles are partitioned into 3 size classes: a sub-micron (diameters < 1 μm), a micron (diam. between 1 and 10 μm) and a super-micron class (> 10 μm diam.). This treatment using modes is computationally much more efficient compared to a bin-scheme (Schulz et al., 1998). Furthermore, to account for the diversity in chemical composition, hygroscopicity, and mixing state, we distinguish between soluble and insoluble modes. In both sub-micron and micron-size, soluble and insoluble aerosols are treated separately. Sea-salt, SO_4 and methane sulfonic acid (MSA) are treated as soluble components of the aerosol. Dust is treated as insoluble, whereas black carbon (BC) and particulate organic matter (POM) appear both in the soluble or insoluble fractions. The aging of primary insoluble carbonaceous particles transfers insoluble aerosol number and mass to soluble with a half-life of 1.1 days (Cooke and Wilson, 1996; Chung et al., 2002).

The uptake and loss of water from aerosol particles is generally fast and depends on the chemical composition, size and surface properties of the aerosol particle. Aerosol water is responsible for about 50% of the global aerosol column loads. This water uptake modifies the aerosol optical properties. The nondimensional optical depth, τ, can be expressed as a function of the effective radius of the aerosol ($\tau = 3\ Q\ M\ /\ 4\ \rho\ r_e$) where Q is the nondimensional extinction coefficient, computed using Mie theory, M, is the aerosol burden per unit area (kg m^{-2}), ρ is the particle density (kg m^{-3}), and r_e, the effective radius (m). As relative humidity increases, this equation must be modified to account for the presence of water. The density is then recomputed as the mass-weighted sum of the dry density of the aerosol and the density of water. The refractive index, hence the extinction, is also changed to account for water. We use a formulation first implemented by Chin et al. (2002) to rewrite the relationship above as a function of the aerosol dry burden M_{dry} (in kg m^{-2}) $\tau = \beta\ M_{dry}$, where β, the specific extinction ($m^2\ kg^{-1}$), is computed as $\beta = 3\ Q\ M\ /\ 4\ \rho\ r_e\ M_{dry}$. The optical properties and hygroscopic growth of sea-salt were taken from Irshad et al. (2005). For sulfates, we followed the relationships published for ammonium sulfate by Martin et al.

(2003). In the case of black carbon and organic carbon we took the same dependence of hygroscopic growth on relative humidity as Chin et al (2002).
The aerosol scheme is thoroughly explained in Schulz (2007) and Balkanski (2011). The chemistry of ammonia/nitrate/ammonium containing aerosols was not considered in this model version.

1.1. LMDz-OR-INCA Set-up

The LMDz-OR-INCA simulations consist of two groups: a simulation covering the historical 1850-2000 period and a set of simulations covering four future projections of emissions for the 2000-2100 period. For the simulation aiming to represent the evolution of tropospheric composition over the past period, the emissions provided by Lamarque et al. (2010) for anthropogenic (including ship and aircraft) and biomass burning emissions are used. These emission datasets consist of fluxes for each decade of methane, carbon monoxide, nitrogen oxides and 23 non-methane hydrocarbons (specific species or family of compounds) for ozone precursors and black carbon, organic carbon, ammonia and sulfur dioxide for aerosols and aerosol precursors. They have a 0.5°x0.5° horizontal resolution.

In order to use the emission fluxes in the INCA model, we reported the individual hydrocarbon fluxes on INCA species or surrogate species as described in Folberth et al. (2006), we spatially interpolated the fluxes to the model resolution (3.75°x1.9°) and we applied a linear interpolation between decades. The methane oxidation is computed interactively according to the emissions and not prescribed on concentrations as often made in such exercises (e.g. Stevenson et al., 2006). The anthropogenic and biomass-burning fluxes, compiled by Lamarque et al. (2010), are added to natural fluxes used in the INCA model. All natural emissions are kept at their present-day levels, except lightning NOx,. Hence, for organic aerosols, the secondary organic matter formed from biogenic emissions is equal to that provided by the AEROCOM emission dataset (Dentener et al., 2006b). The lightning NOx emissions are computed interactively during the simulations depending on the convective clouds, according to Price and Rind (1992), with a vertical distribution based on Pickering et al. (1998) as described in Jourdain & Hauglustaine (2001). The ORCHIDEE vegetation model was used (offline) to calculate biogenic surface fluxes of isoprene, terpenes, acetone and methanol as well as NO soil emissions as described by Lathière et al. (2006). Natural emissions of dust and sea salt are computed using the 10 m wind components from the ECMWF reanalysis for 2006 and, consequently, have seasonal cycles, but no inter-annual variability. As described in Hauglustaine et al. (2004), the stratospheric ozone concentrations are relaxed toward observations at the altitudes having potential temperatures above 380K. The ozone observations are taken from the monthly mean 3D climatologies of Li and Shine [1995], based on ozone soundings and different satellite data.

The LMDz general circulation model requires sea surface temperature (SST), solar constant and LL-GHG global mean concentrations as forcings. For historical simulations, we use the HADiSST for sea surface temperature (Rayner et al. 2003) and the evolution of LL-GHG concentrations compiled in the AR4-IPCC report. For future projections, we use the LL-GHG concentrations distributed by the RCP database. No RCP projections from Earth System Model were available at that time. The SST are from previous IPSL-CM4 simulations having similar climate trajectories in terms of radiative forcing evolution. Hence, for the RCP8.5 projection, we use the SST from IPSL-CM4 simulation for the SRES-A2 scenario. Analogously, we use the SRES-A1B for RCP6.0, the SRES-B1 for RCP4.5 and the scenario E1 (van Vuuren et al. 2007) for the RCP2.6 simulation.
Using the model set-up described above, the LMDz-OR-INCA is run to generate 3D monthly fields of ozone volume mixing ratio and aerosol loads (for SO_4, POM, SS, DUST and BC)

with a 3.75x1.9° horizontal resolution over 19 vertical levels. In these simulations, the tropospheric composition simulated by INCA does not influence the climate simulated by LMDz-OR.

11. MIROC-CHEM

MIROC-ESM-CHEM is an atmospheric chemistry coupled version of the earth system model MIROC-ESM [Watanabe et al., 2011]. Atmospheric chemistry component in MIROC-ESM-CHEM is based on that used in the chemistry model CHASER [Sudo et al., 2002; Sudo and Akimoto, 2007] which considers the detailed photochemistry in the troposphere, wet and dry deposition of chemical species, and emissions of primary chemical species from a variety of sources. For MIROC-ESM-CHEM, the chemistry of CHASER has been extended to include the stratosphere by incorporating halogen chemistry and related processes based on the schemes used in the CCSR/NIES stratospheric chemistry model [Akiyoshi et al., 2004]. In the configuration for the CMIP5 simulations, the model calculates the concentrations of 92 chemical species with 262 chemical reactions (58 photolytic, 183 kinetic, and 21 heterogeneous reactions) at approximately 2.8° by 2.8° (T42) horizontal resolution with 80 vertical layers up to 0.003 hPa. The model considers the fundamental chemical cycle of O_x-NO_x-HO_x-CH_4-CO with oxidation of NMVOCs (ethane, ethane, propane, propene, butane, acetone, methanol, isoprene, and terpenes) to properly represent the ozone chemistry in the troposphere. The emission of NO_x from lightning is calculated in conjunction with the convection scheme of the MIROC-ESM and accordingly can vary year to year responding to the interannual variability and climatic trends. Biogenic emissions of VOCs, such as isoprene or terpenes, are considered in the model, but are not linked to the vegetation processes in the models so far. The model includes detailed stratospheric chemistry which calculates the chlorine- and bromine-containing compounds as well as CFCs, HFCs, OCS, and N_2O. The formation of PSCs and associated 13 heterogeneous reactions on their surfaces are calculated. The photolysis rates (J-values) are calculated on-line using temperature and actinic fluxes computed in the radiation component [Sekiguchi and Nakajima, 2008] considering absorption and scattering by gases, aerosols, and clouds as well as the effect of surface albedo. In MIROC-ESM-CHEM, influences of short-wave radiative forcing associated with the solar cycle (spectral forcing recommended by SOLARIS), volcanic eruptions (based on Sato et al. [1993]), and subsequent changes in stratospheric ozone are also taken into account for the calculation of the photolysis rate. The calculated concentrations of oxidants (ozone, OH, and H_2O_2) are input into the tropospheric aerosol module in MIROC-ESM, SPRINTARS [Takemura et al., 2000, 2002, 2005], to calculate the sulfate aerosol formation from oxidation of SO_2 and DMS.

12. MOCAGE

MOCAGE (Modèle de Chimie Atmosphérique de Grande Echelle) is Météo-France's Chemical Transport Model. The version used in ACCMIP uses a more complex tropospheric chemistry than that described in [Teyssèdre et al, 2007]. MOCAGE combines the RACM [Stockwell et al, 1997] tropospheric scheme and the REPROBUS [Lefèvre et al, 1994] stratospheric one, consistently applied from the surface to the model top.

It takes 119 gaseous species into account (no aerosols), that can be grouped in families, with 91 being transported. In the stratosphere, 9 heterogeneous reactions are described, using the parameterization of [Carlslaw et al, 1995]. Moreover, 52 photolysis and 312 thermal reactions are described. The photolysis rates follow look-up tables and are modified to account for cloudiness, following [Chang et al, 1987] . The model includes a reaction pathway for HO2 + NO to yield HNO3 [Butkovskaya et al., 2007].

The resolution of the model is 2x2 degree on a regular grid, with 47 levels from the ground up to 5hPa. For each ACCMIP simulation, four years were kept after 1 year of spin-up. The meterological forcing is taken from the CNRM-CM model, which was used for CMIP5 simulations [Voldoire et al, 2012]. However, convection is recomputed following [Bechtold et al, 2001]'s parameterization. Convective in-cloud scavenging is determined in the updraft [Mari et al, 2000], whereas wet deposition due to stratiform precipitations follow [Giorgi and Chameides, 1986]. A one-year simulation has been performed to compute dry deposition velocities following Wesely's approach. Values have been averaged to get monthly diurnal profiles. The same values have been used for all simulations.

Except lightning NOx, natural emissions are monthly mean distributions kept constant throughout all simulations.. Details about the origin of these natural emissions can be found in [Teyssèdre et al, 2007]. Natural soil-NOx emissions are of 4.5 TgN/yr, isoprene 568 Tg/yr, and other VOCs 406Tg of C/yr. LiNOx are paramerized in the convection scheme following [Price and Rind, 1997], and are hence climate-sensitive, but the range of global emissions is small : from 5TgN/yr in the 1850s to 6.3TgN/yr in the 2100s with the RCP8.5 climate conditions. Methane concentrations were prescribed at the surface following a monthly zonal climatology taking the evolution of the global value as a function of RCPs into account.

13. NCAR-CAM3.5

We use the global three-dimensional Community Atmosphere Model version 3.5 (Gent et al., 2009) modified to include interactive chemistry (Lamarque et al., 2012) to calculate distributions of gases and aerosols in the troposphere and the lower to mid-stratosphere. The model configuration includes a horizontal resolution of 1.9^{o} (latitude) by 2.5^{o} (longitude) and 26 hybrid levels, from the surface to ≈ 40 km with a timestep of 30 minutes. In order to simulate the evolution of the atmospheric composition over the model vertical range, the chemical mechanism used in this study is formulated to provide an accurate representation of both tropospheric and stratospheric chemistry (Lamarque et al., 2008). Specifically, to successfully simulate the chemistry above 100 hPa, we include a representation of stratospheric chemistry (including polar ozone loss associated with stratospheric clouds) from version 3 of MOZART (MOZART-3; Kinnison et al., 2007). The tropospheric chemistry mechanism has a simplified representation of non-methane hydrocarbon chemistry in addition to standard methane chemistry, extended from Houweling et al. (1998) with the inclusion of isoprene and terpene oxidation and updated to JPL-2006 (Sander et al., 2006). This model has a representation of aerosols based on the work by Tie et al. (2001, 2005); i.e., sulfate aerosol is formed by the oxidation of SO_2 in the gas phase (by reaction with the hydroxyl radical) and in the aqueous phase (by reaction with ozone and hydrogen peroxide). Furthermore, the model includes a representation of ammonium nitrate that is dependent on the amount of sulfate present in the air mass following the parameterization of gas/aerosol partitioning by Metzger et al. (2002). Because only the bulk mass is calculated, a lognormal distribution is assumed for all aerosols using different mean radius and geometric standard deviation (Liao et al., 2003). We use a 1.6 days of exponential lifetime for the conversion from hydrophobic to hydrophilic carbonaceous aerosols (organic and black). Natural aerosols (desert dust and sea salt) are implemented following Mahowald et al. (2006a and b), and the sources of these aerosols are derived based on the model-calculated wind speed and surface conditions.

At the lower boundary, the time-varying (monthly values) zonal-averaged distributions of CO_2, CH_4, H_2, N_2O and all the halocarbons (CFC-11, CFC-12, CFC-113, HCFC-22, H-1211, H-1301, CCl_4, CH_3CCl_3, CH_3Cl and CH_3Br) are specified following the datasets described in Meinshausen et al. (2011), except for H_2 which is kept at a constant 500 ppbv. The natural emissions of ozone precursors and of sulfur compounds (from non-eruptive volcanoes, Dentener et al., 2006) are kept constant (i.e. set at their value in 2000) for the whole duration of the simulations.

As no climate model simulations forced by the RCPs were available at the time simulations in support of CCSM4 (Gent et al., 2011; Lamarque et al., 2010 and 2011) were performed, we have used previously generated monthly-mean time-varying sea-surface temperatures (SSTs) and sea-ice distributions using analogous (see Table 1) AR4 simulations by CCSM-3 (Meehl et al., 2007). The choice of the closest analogue to the Supplemental Report on Emission Scenarios (SRES)-based climate simulations is driven by its estimated total radiative forcing at 2100 (Meehl et al., 2007), as discussed in Lamarque et al. (2011).

14. NCAR-CAM5.1

NCAR-CAM5.1 is version 5.1 of the Community Atmosphere Model. Aerosols in CAM5 are represented by three internally-mixed log-normal modes (Aiken, accumulation, and coarse), with the total number mixing ratio and the mass mixing ratio of each component (sulfate, organic carbon, black carbon, mineral dust and sea salt) predicted for each mode (Liu et al., 2012). Anthropogenic emissions of SO_2, black carbon and organic carbon are from Lamarque et al. (2010). Natural emissions are prescribed for DMS, volcanic SO_2, and volatile organics, and are calculated on-line for mineral dust and sea salt (Liu et al., 2012). DMS is oxidixed by OH and NO_3 to form SO_2, which is oxidized by OH in air and by H_2O_2 and O_3 in cloud water. Concentrations of the oxidants O_3, OH, HO_2, and NO_3 are interpolated from monthly means simulated by CAM-Chem (Lamarque et al., 2010), while H_2O_2 production and loss are calculated in CAM5.1. Volatile organics are instantaneously oxidized with prescribed yields to form semi-volatile organic, which condenses on the aerosol modes (Liu et al., 2012). Water uptake is treated using Kohler theory with volume mean hygroscopicity, and aerosol optical properties are parameterized of Mie calculations assuming volume mixing of refractive indices (Ghan and Zaveri, 2007). Stratiform cloud microphysics is represented using the Morrison and Gettelman (2008) double-moment scheme for droplets, crystals, rain and snow (Liu et al., 2007; Gettelman et al., 2008, 2010), and stratiform cloud macrophysics is described by Park et al. (2012). The treatments of shallow and deep cumulus clouds are described by Park and Bretherton (2009) and Zhang and McFarlane (1995), respectively. The turbulence treatment is described by Bretherton and Park (2009). Radiative transfer is calculated using the Rapid Radiative Transfer Model for GCMs (RRTMG) scheme (Iacono et al. 2008). The ACCMIP simulations by CAM5.1 were not constrained by atmospheric observations, but ocean surface conditions were taken from coupled simulations by the Community Climate System Model (Gent et al., 2009). The finite-volume dynamical core (Lin and Rood 1996; Lin 2004) is used, with a horizontal resolution of 1.9° latitude, 2.5° longitude, and 30 layers. The decomposition of aerosol radiative forcing is described by Ghan et al. (2012)

15. STOC-HadAM3

STOC-HadAM3 comprises the STOCHEM Lagrangian tropospheric chemistry transport model [Collins et al., 1997; Stevenson et al., 2004] coupled to the Hadley Centre atmospheric climate model HadAM3 [Pope et al., 2000]. Multiple meteorological fields are passed from HadAM3 to STOCHEM to drive advective, convective, and other physical processes. There is no feedback from the chemistry to the climate model. Within STOCHEM the atmosphere is divided into 100 000 equal mass air parcels which are transported by the HadAM3 winds. For output the STOCHEM fields are mapped onto a 5 x 5 degree latitude-longitude grid with 19 hybrid sigma pressure levels from the surface up to 50 hPa with each layer containing an approximately equal mass of air. HadAM3 has resolution 2.5 x 3.75 in latitude and longitude with 19 hybrid pressure levels up to 5 hPa. Sea-surface temperature and sea-ice boundary conditions for HadAM3 were annually-repeating decadal means taken from the appropriate years and scenario of HadGEM2 CMIP5 simulations [Jones et al., 2011]. Seven month's model spin-up was allowed prior to the analysis period.

The STOCHEM tropospheric chemistry scheme [Collins et al.. 2000] contains 70 species including SOx, NOy and NHx aerosols. Eleven non-methane volatile organic compounds and their oxidation products are treated. Methane concentrations were fixed globally at the CMIP5-recommended value for the simulation time slice [http://www.iiasa.ac.at/web-apps/tnt/RcpDb/dsd?Action=htmlpage&page=download#]. There are 174 photolytic and thermal reactions, including 19 aqueous-phase and one heterogeneous reaction. Above the tropopause the model ozone is relaxed towards the AC&C/SPARC ozone climatology [Cionni et al., 2001]. No stratospheric chemistry is included. The 17 photolysis rates are calculated interactively by the 1-D, two-stream method of Hough [1988], accounting for the modelled cloud distribution and using a prescribed aerosol loading (same for all simulations). The ozone column above the model top is taken from the AC&C/SPARC climatology. Rate coefficient data are mainly from Sander et al, 2006.

Dry deposition rates for all species are calculated with a resistance analogy scheme, with inputs of land-surface type, species-dependent deposition velocities, boundary-layer height, and an effective vertical eddy diffusion coefficient derived from the surface stress, heat flux, and temperature [Sanderson et al., 2003]. Wet deposition rates use species-dependent scavenging coefficients from Penner et al., [1994], and vary between dynamic and convective precipitation [Stevenson et al., 2003].

Natural emissions of isoprene are calculated from modelled photosynthetically active radiation (PAR) flux density and temperature using a scheme based on Guenther et al., [1995]. Lightning NOx production is calculated interactively according to the modelled cloud height [Price and Rind, 1992, Price et al., 1997.] Soil NOx emission is fixed at 5.6 Tg N/year for all simulations [Yienger and Levy, 1995]. Natural emissions (vegetation, soil and ocean) of other species were also fixed at the same value for all simulations and largely taken from IPCC AR4 WG1 [2007].

The air parcels within STOCHEM are advected by a Runge-Kutta fourth order method with random displacements added to the parcels based on locally prescribed diffusivities [Collins et al., 1997]. Convective diagnostics from HadAM3 are used to derive the probability of a parcel being subject to convective transport [Collins et al. 2002]. Inter-parcel mixing is parameterised by relaxing the mixing ratios in each parcel to the background average of all local parcels. Within the boundary layer the vertical position of each parcel is randomly reassigned at each time step while allowing some parcels to escape the boundary layer to balance entrainment from above [Stevenson et al. 1998].

STOC-HadAM3 participated in the Task Force on Hemispheric Transport of Air Pollution modelling exercise [TF-HTAP, 2010] and, in a variety of comparisons, was generally fairly central in the multi-model spread.

16. UM-CAM

UM_CAM is based on the UK Met Office Unified Model version 4.5 combined with a detailed tropospheric chemistry scheme [e.g., Zeng et al., 2008, 2010]. It has 19 levels from the surface to 4.6 hPa with 6 levels above 150 hPa. Its horizontal resolution is 3.75° by 2.5°. The model uses prescribed sea surface temperatures (SSTs) and sea ice fields.

Sea surface temperature and sea ice fields are from the UKMO CMIP5 HadGEM2 simulations and are decadal means. For each scenario the model runs 10 years with a 4-month spin-up.

There are 60 chemical species and 174 gas phase reactions in the model. Loss of trace species by dry deposition and the deposition velocities are calculated using prescribed deposition velocities at 1m height, depending on season, time of the day and on the type of surface (grass, forest, dessert, water, snow/ice) and are extrapolated to the middle of the lowest model layer using a formula described by Sorteberg and Hov (1996). Wet deposition of soluble species is represented as a first order loss using model-calculated large-scale and convective rainfall rates described by Giannakopoulos et al. (1999). We have no explicit stratospheric chemistry in the model, instead, offline stratospheric O_3 (from the CMIP5 dataset) is prescribed above 100 hPa between 50^{O}S-50^{O}N and above 150 poleward of 50^{O}. The model uses the diurnal varying photolysis rates calculated off-line in a 2-D model (Law and Pyle, 1993) and interpolated to 3-D fields. The effect of changes in cloudiness is not included.

Natural emissions include soil NO_x emission (7 TgN/yr), CO oceanic and biogenic emissions (total 100 Tg CO/yr) and isoprene emissions (390 Tg/yr). Lightning NO_x emissions are calculated in the model using parameterization from Price and Rind (1992, 1994).

The model's advection scheme is monotonic, conservative, and based on the one-dimensional NIRVANA scheme (Leonard et al., 1995), extended to/spherical geometry. Convection is parameterized by a penetrative mass flux scheme (Gregory and Rowntree, 1990) in which buoyant parcels are modified by entrainment and detrainment to represent an ensemble of convective clouds.

References

Akiyoshi, H., T. Sugita, H. Kanzawa, and N. Kawamoto (2004), Ozone perturbations in the Arctic summer lower stratosphere as a reflection of NOX chemistry and planetary scale wave activity, *J. Geophys. Res*., **109**, D03304, doi:10.1029/2003JD003632.

Allen, D. J. and K. E. Pickering, Evaluation of lightning flash rate parameterizations for use in a global chemical transport model, *J. Geophys. Res*., **107**, doi:10.1029/2002JD002066, 2002.

Arneth, A., Ü. Niinemets, S. Pressley, J. Bäck, P. Hari, T. Karl, S. Noe, I. C. Prentice, D. Serça, T. Hickler, A. Wolf, B. Smith (2007), Process-based estimates of terrestrial ecosystem isoprene emissions: incorporating the effects of a direct CO2–isoprene interaction, *Atmospheric Chemistry and Physics*, 7, 31–53.

Austin, J., and Wilson, J.: Sensitivity of polar ozone to sea surface temperatures and halogen amounts, J. Geophys. Res., 115, D18303, doi:10.1029/2009JD013292, 2010.

Bauer, S.E., D. Koch, N. Unger, S.M. Metzger, D.T. Shindell, and D.G. Streets, 2007: Nitrate aerosols today and in 2030: Importance relative to other aerosol species and tropospheric ozone. Atmos. Chem. Phys., 7, 5043-5059, doi:10.5194/acp-7-5043-2007.

Bechtold, P., Bazile, E., Guichard, F., Mascart, P., and Richard, E.: A mass flux convection scheme for regional and global models, Q. J. Roy. Meteor. Soc., 127, 869–886, 2001.

Bellouin, N., J. Rae, A. Jones, C. Johnson, J. Haywood, and O. Boucher (2011), Aerosol forcing in the Climate Model Intercomparison Project (CMIP5) simulations by HadGEM2-ES and the role of ammonium nitrate, J. Geophys. Res., 116, D20206, doi:10.1029/2011JD016074.

Berglen, T. F., Berntsen, T. K., Isaksen, I. S. A. and Sundet, J. K.: A global model of the coupled sulfur/oxidant chemistry in the troposphere: The sulfur cycle, J. Geophys. Res., 109(D19), D19310, 2004.

Berntsen, T. K. and Isaksen, I. S. A.: A global three-dimensional chemical transport model for the troposphere .1. Model description and CO and ozone results, Journal of Geophysical Research-Atmospheres, 102(D17), 21239-21280, 1997.

Bey I., Jacob, D. J., Yantosca, R. M., Logan, J. A., Field, B., Fiore, A. M., Li, Q., Liu, H., Mickley, L. J., and Schultz, M.: Global modeling of tropospheric chemistry with assimilated meteorology: Model description and evaluation, J. Geophys. Res., 106, 23,073-23,096, 2001

Bian, H., and M. Prather (2002), Fast-J2: Accurate simulations of photolysis in global climate models, J. Atmos. Chem., 41, 281-296.

Bretherton, C. S. and S. Park, 2009: A new moist turbulence parameterization in the community atmosphere model. J. Climate, 22(12): 3422-3448 DOI 10.1175/2008jcli2556.1.

Butkovskaya, N., A. Kukui, and G. Le Bras (2007), HNO3 Forming Channel of the HO2 + NO Reaction as a Function of Pressure and Temperature in the Ranges of 72-600 Torr and 223-323 K J. Phys. Chem. A, 111, 9047-9053.

Cagnazzo C., Manzini, E., Giorgetta, M. A., Forster, P. M. De F., and Morcrette, J. J.: Impact of an improved shortwave radiation scheme in the MAECHAM5 General Circulation Model, Atmos. Chem. Phys., 7, 2503-2515, 2007. Cionni, I., V. Eyring, J. F. Lamarque, W. J. Randel, D. S. Stevenson, F. Wu, G. E. Bodeker, T. G. Shepherd, D. T. Shindell, and D. W. Waugh, Ozone database in support of CMIP5 simulations: results and corresponding radiative forcing, Atmos. Chem. Phys. Discuss., 11, 10875-10933, doi:10.5194/acpd-11-10875-2011, 2011.

Cameron-Smith, P., J. F. Lamarque, P. Connell, C. Chuang, and F. Vitt, Toward an Earth system model: atmospheric chemistry, coupling, and petascale computing, in Scidac 2006: Scientific Discovery through Advanced Computing, edited by W. M. Tang, pp. 343-350., 2006

Cariolle, D., A. Lasserre-Bigorry, J.-F. Royer, and J.-F. Geleyn , A General Circulation Model Simulation of the Springtime Antarctic Ozone Decrease and Its Impact on Mid-Latitudes, J. Geophys. Res., 95(D2), 1883–1898, doi:10.1029/JD095iD02p01883, 1990

Carslaw, K. S., Luo, B. P., and Peter, T.: An analytic expression for the composition of aqueous HNO3-H2SO4 stratospheric aerosols including gas phase removal of HNO3, Geophys. Res. Lett., 22, 1877-1880, 1995.

Chang, J. S., Brost, R. A., Isaksen, I. S. A., Madronich, S., Middleton, P., Stockwell, W. R. and Walcek, C. J., A three-dimensional Eulerian acid deposition model: Physical concepts and formulation, J. Geophys. Res., 92, 14681-14700, 1987.

Collins, W. J., D. S. Stevenson, C. E. Johnson, and R. G. Derwent (1997), Tropospheric ozone in a global-scale three-dimensional Lagrangian model and its response to NOx emission controls, J. Atmos. Chem., 26, 223– 274.

Collins, W. J., N. Bellouin, M. Doutriaux-Boucher, N. Gedney, P. Halloran, T. Hinton, J. Hughes, C. D. Jones, M. Joshi, S. Liddicoat, G. Martin, F. O'Connor, J. Rae, C. Senior, S. Sitch, I. Totterdell, A. Wiltshire, and S. Woodward, Development and evaluation of an Earth-system model - HadGEM2, Geosci. Model Dev. 4 (2011) pp. 1051-1075.

Collins, W. J., R. G. Derwent, C. E. Johnson, and D. S. Stevenson (2002), A comparison of two schemes for the convective transport of chemical species in a Lagrangian global chemistry model, Q. J. R. Meteorol. Soc., 128, 991– 1009.

Collins, W. J., Stevenson, D. S., Johnson, C. E., and Derwent, R. G., 2000: The European regional ozone distribution and its links with the global scale for the years 1992 and 2015, Atmos. Environ. 34, 255–267.

Davies, T., M.J.P. Cullen, A.J. Malcom, M.H. Mawson, A. Staniforth, A.A. White, and N. Wood, A new dynamical core for the Met Office's global and regional modelling of the atmosphere, Q.J.R. Meteorology Soc., 131, pp. 1759-1782, 2005.

Dentener, F, S. Kinne, T. Bond, O. Boucher, J. Cofala, S. Generoso, P. Ginoux, S. Gong, J. J. Hoelzemann, A. Ito, L. Marelli, J. E. Penner, J.-P. Putaud, C. Textor, M. Schulz, G. R. van der Werf, and J. Wilson : Emissions of primary aerosol and precursor gases in the years 2000 and 1750 prescribed data-sets for AeroCom, Atmospheric Chemistry and Physics, 6, 4321-4344, 2006.

Donner, L.J., Wyman, B.L., Hemler, R.S., Horowitz, L.W., Ming, Y., Zhao, M., Golaz, J.-C., Ginoux, P., Lin, S.-J., Schwarzkopf, M.D., Austin, J., Alaka, G., Cooke, W.F., Delworth, T.L., Freidenreich, S.M., Gordon, C.T., Griffies, S.M., Held, I.M., Hurlin, W.J., Klein, S.A., Knutson, T.R., Langenhorst, A.R., Lee, H.-C., Lin, Y., Magi, B.I., Malyshev, S.L., Milly, P.C., Naik, V., Nath, M.J., Pincus, R., Ploshay, J.J., Ramaswamy, V., Seman, C.J., Shevliakova, E., Sirutis, J.J., Stern, W.F., Stouffer, R.J., Wilson, R.J., Winton, M., Wittenberg, A.T., Zeng, F.: The dynamical core, physical parameterizations, and basic simulation characteristics of the atmospheric component of the GFDL global coupled model CM3, J. Climate, 24, 3484–3519, doi: /dx.doi.org/10.1175/2011JCLI3955, 2011.

Duncan, B.N., S.E. Strahan, Y. Yoshida, S.D. Steenrod , and N. Livesey (2007), Model study of the cross-tropopause transport of biomass burning pollution, Atmos. Chem. Phys., 7, 3713-3736.

Emmons, L. K., Walters, S., Hess, P. G., Lamarque, J.-F., Pfister, G. G., Fillmore, D., Granier, C., Guenther, A., Kinnison, D., Laepple, T., Orlando, J., Tie, X., Tyndall, G., Wiedinmyer, C., Baughcum, S. L., and Kloster, S.: Description and evaluation of the Model for Ozone and related chemical Tracers, version 4 (MOZART-4), Geosci. Model Dev., 3, 43-67, 2010.

Fang, Y., Fiore, A. M., Horowitz, L. W., Gnanadesikan, A., Held, I., Chen, G., Vecchi, G., and Levy II, H.: The impacts of changing transport and precipitation on pollutant distributions in a future climate, J. Geophys. Res., 116, D18303, doi:10.1029/2011JD015642, 2011.

Fichefet, T. and Morales-Maqueda, M.A. (1997): Sensitivity of a global sea ice model to the treatment of ice thermodynamics and dynamics. J. Geophys. Res. 102, 12,609 – 12,646.

Fogli, P.G. and Coauthors, 2009: INGV-CMCC Carbon: A Carbon Cycle Earth System Model, CMCC online RP0061: http://www.cmcc.it/publications-meetings/publications/research-papers/rp0061-ingvcmcc-carbon-icc-a-carbon-cycle-earth-system-modelhttp://www.cmcc.it/publicationsmeetings/publications/research-papers/rp0061-ingv-cmcc-carbon-icc-a-carbon-cycle-earth-systemmodel

Ganzeveld, L., van Aardenne, J., Butler, T., Lawrence, M., Metzger, S., Stier, P., Zimmermann, P., and Lelieveld, J.: Technical Note: Anthropogenic and natural offline emissions and the online EMissions and dry DEPosition submodel EMDEP of the Modular Earth Submodel system (MESSy), Atmos. Chem. Phys. Discuss., 6, 5457-5483, 2006.
Gent, P. R., G. Danabasoglu, L. J. Donner, M. M. Holland, E. C. Hunke, S. R. Jayne, D. M. Lawrence, R. B. Neale, P. J. Rasch, M. Vertenstein, P. H. Worley, Z. -L. Yang, and M. Zhang, 2011: The Community Climate System Model version 4. J. Climate, 24, 4973-4991, doi: 10.1175/2011JCLI4083.1.

Gent, P. R., Yeager, S. G., Neale, R. B., Levis, S., and Bailey, D. A.: Improvements in a half degree atmosphere/land version of the CCSM, Clim. Dynam., 79, 25–58, doi:10.1007/s00382-009- 0614-8, 2009.

Gettelman, A., H. Morrison and S. J. Ghan, 2008: A new two-moment bulk stratiform cloud microphysics scheme in the community atmosphere model, version 3 (CAM3). Part II:

Single-colunm and global results. J. Climate, 21(15): 3660-3679 DOI Doi 10.1175/2008jcli2116.1.

Gettelman, A., X. Liu, S. J. Ghan, H. Morrison, S. Park, A. Conley, S. A. Klein, J. Boyle, D. Mitchell, and J-L F Li, 2010: Global simulations of ice nucleation and ice supersaturation with an improved cloud scheme in the community atmosphere model. J. Geophys. Res., 115(D18216), doi:10.1029/2009JD013797.

Ghan, S. J. and R. A. Zaveri, 2007: Parameterization of optical properties for hydrated internally mixed aerosol. J. Geophys. Res., 112(D10): - DOI D10201, 10.1029/2006jd007927.

Ghan, S. J., X. Liu, R. C. Easter, R. Zaveri, P. J. Rasch, J.-H. Yoon, and. B. Eaton, 2012: Toward a minimal representation of aerosols in climate models: Comparative decomposition of aerosol direct, semi-direct and indirect radiative forcing. J. Climate, doi: 10.1175/JCLI-D-11-00650.1, in press.

Giannakopoulos, C, M.P. Chipperfield, K.S. Law, and J.A. Pyle, Validation and intercomparison of wet and dry deposition schemes using 210Pb in a global 3D offline chemistry model, J.G.R, 104, D19, pp. 23,761-23784, 1999.

Giorgi, F. and W. L. Chameides, Rainout lifetimes of highly soluble aerosols and gases as inferred from simulations with a General Circulation Model, J. Geophys. Res., 91, 14367-14376, 1986.

Granier, C., Guenther, A., Lamarque, J.-F., Mieville, A., Muller, J., Olivier, J., Orlando, J., Peters, J., Petron, G., Tyndall, G., and Wallens, S.: POET, a database of surface emissions of ozone precursors, available at: http://www.aero.jussieu.fr/projet/ACCENT/POET.php, 2005

Granier, C., J. F. Lamarque, A. Mieville, J. F. Muller, J. Olivier, J. Orlando, J. Peters, G. Petron, G. Tyndall, and S. Wallens: POET, a database of surface emissions of ozone precursors. Available on internet at http://www.aero.jussieu.fr/projet/ACCENT/POET.php, 2005.

Gregory, D., and P.R. Rowntree, A mass flux scheme with representation of cloud ensemble characteristics and stability-dependent closure, Mon. Wea. Rev., 118, 1483-1506, 1990.

Grewe, V., Brunner, D., Dameris, M., Grenfell, J. L., Hein, R., Shindell, D., and Staehelin, J.: Origin and variability of upper tropospheric nitrogen oxides and ozone at northern mid-latitudes, Atmos. Environ., 35, 3421-3433, 2001.

Griffies., S. M., Winton, M., Donner, L. J., Horowitz, L. W., Downes, S. M., Farneti, R., Gnanadesikan, A., Hurlin, W. J., Lee, H. C., Liang, Z., Palter, J. B., Samuels, B. L., Wittenberg, A. T., Wyman, B., Yin, J., and Zadeh, N.: The GFDL CM3 coupled climate model: characteristics of the ocean and sea ice simulations, J. Clim., 24, doi: 10.1175/2011JCLI3964.1, 2011.

Grini, A., Myhre, G., Sundet, J. K. and Isaksen, I. S. A.: Modeling the annual cycle of sea salt in the global 3D model Oslo CTM2: Concentrations, fluxes, and radiative impact, Journal Of Climate, 15(13), 1717-1730, 2002.

Grini, A., Myhre, G., Zender, C. S. and Isaksen, I. S. A.: Model simulations of dust sources and transport in the global atmosphere: Effects of soil erodibility and wind speed variability, Journal Of Geophysical Research-Atmospheres, 110(D2), D02205, 2005.

Guenther, A., B. Baugh, G. Brasseur, J. Greenberg, P. Harley, L. Klinger, D. Serça, and L. Vierling (1999), Isoprene emission estimates and uncertainties for the Central African EXPRESSO study domain, J. Geophys. Res., 104(D23), 30,625–30,639, doi:10.1029/1999JD900391.

Guenther, A., C. N. Hewitt, D. Erickson, R. Fall, C. Geron, T. Graedel, P. Harley, L. Klinger, M. Lerdau, W. A. Mckay, T. Pierce, B. Scholes, R. Steinbrecher, R. Tallamraju, J. Taylor, P.Zimmerman (1995), A global model of natural volatile organic compound emissions, J. Geophys. Res., 100(D5), 8873–8892, doi:10.1029/94JD02950.

Hanson, D. R., and Mauersberger, K.: Laboratory studies of nitric acid trihydrate: implications for the south polar stratosphere, Geophys. Res. Lett., 15, 855-858, 1988.

Holtslag, A. A. M., Debruijn, E. I. F. and Pan, H. L.: A High-Resolution Air-Mass Transformation Model For Short-Range Weather Forecasting, Monthly Weather Review, 118(8), 1561-1575, 1990.

Horowitz, L. W., Fiore, A. M., Milly, G. P., Cohen, R. C., Perring, A., Wooldridge, P. J., Hess, P. G., Emmons, L. K., and Lamarque, J.-F.: Observational constraints on the chemistry of isoprene nitrates over the eastern Unites States, J. Geophys. Res., 112 D12S08, doi:10.1029/2006JD007747, 2007.

Horowitz, L. W.: Past, present, and future concentrations of tropospheric ozone and aerosols: methodology, ozone evaluation and sensitivity to aerosol wet removal, J. Geophys. Res., 111, D22211, doi:10.1029/2005JD006937, 2006.

Horowitz, L. W., Walters, S., Mauzerall, D. L., Emmons, L. K., Rasch, P. J., Granier, C., Tie, X., Lamarque, J.-F., Schultz, M. G., Tyndall, G. S., Orlando, J. J., and Brasseur, G. P.: A global simulation of tropospheric ozone and related tracers: description and evaluation of MOZART, version 2, J. Geophys. Res., 108, D24, 4784, doi:10.1029/2002JD002853, 2003.

Hough, A.M., The calculation of photolysis rates for use in global tropospheric modelling studies, AERE Report, 13,259, At. Energy Res. Estab., Harwell, U.K., 1988

Houweling, S., F. Dentener, and J. Lelieveld, The impact of non-methane hydrocarbon compounds on tropospheric photochemistry, J. Geophys. Res., 103, 10,673–10,696, doi:10.1029/97JD03582, 1998.

Hoyle, C. R., Berntsen, T., Myhre, G. and Isaksen, I. S. A.: Secondary organic aerosol in the global aerosol - chemical transport model Oslo CTM2, Atmospheric Chemistry and Physics, 7(21), 5675-5694, 2007.

Hoyle, C. R., Myhre, G., Berntsen, T. K. and Isaksen, I. S. A.: Anthropogenic influence on SOA and the resulting radiative forcing, Atmospheric Chemistry and Physics, 9(8), 2715-2728, 2009.

Hsu, J., and M. J. Prather, Stratospheric variability and tropospheric ozone, J. Geophys. Res., 114, D06102, doi:10.1029/2008JD010942. , 2009
http://www.agu.org/journals/jd/jd0906/2008JD010942/2008JD010942.pdf

Hurrell, J.W., J.J. Hack, D. Shea, J.M. Caron, and J. Rosinski (2008), A New Sea Surface Temperature and Sea Ice Boundary Dataset for the Community Atmosphere Model. J. Climate, 21, 5145–5153.

Iacono, M. J., J. S. Delamere, E. J. Mlawer, M. W. Shephard, S. A. Clough and W. D. Collins, 2008: Radiative forcing by long-lived greenhouse gases: Calculations with the AER radiative transfer models. J. Geophys. Res., 113(D13): D13103, Doi 10.1029/2008jd009944.

IPCC AR4 WG1 (2007), Solomon, S.; Qin, D.; Manning, M.; Chen, Z.; Marquis, M.; Averyt, K.B.; Tignor, M.; and Miller, H.L., ed., Climate Change 2007: The Physical Science Basis, Contribution of Working Group I to the Fourth Assessment Report of the Intergovernmental Panel on Climate Change, Cambridge University Press, ISBN 978-0-521-88009-1 (pb: 978-0-521-70596-7).

Jöckel, P., Tost, H., Pozzer, A., Brühl, C., Buchholz, J., Ganzeveld, L., Hoor, P., Kerkweg, A., Lawrence, M. G., Sander, R., Steil, B., Stiller, G., Tanarhte, M., Taraborrelli, D., van Aardenne, J., and Lelieveld, J.: The atmospheric chemistry general circulation model ECHAM5/MESSy1: consistent simulation of ozone from the surface to the mesosphere, Atmos. Chem. Phys., 6, 5067-5104, 2006.

Jöckel, P., Kerkweg, A., Buchholz-Dietsch, J., Tost, H., Sander, R., and Pozzer, A.: Technical Note: Coupling of chemical processes with the Modular Earth Submodel System (MESSy) submodel TRACER, Atmos. Chem. Phys., 8, 1677-1687, doi:10.5194/acp-8-1677-2008, 2008.

John, J., Fiore, A. M., Naik, V., Horowitz, L. W., and Dunne, J. P.: Climate versus emission drivers of methane lifetime from 1860-2100, submitted to Atmos. Chem. Phys, 2012.

Jones, C. D., J. K. Hughes, N. Bellouin, S. C. Hardiman, G. S. Jones, J. Knight, S. Liddicoat, F. M. O'Connor, R. J. Andre2, C. Bell, K.-O. Boo, A. Bozzo, N. Butchart, P. Cadule, K. D. Corbin, M. Doutriaux-Boucher, P. Friedlingstein, J. Gornall, L. Gray, P. R. Halloran, G. Hurtt, W. J. Ingram J.-F. Lamarque, R. M. Law, M. Meinshausen, S. Osprey, E. J. Palin, L. Parsons Chini, T. Raddatz, M. G. Sanderson, A. A. Sellar, A. Schurer, P. Valdes, N. Wood, S. Woodward, M. Yoshioka, and M. Zerroukat: The HadGEM2-ES implementation of CMIP5 centennial simulations. Geosci. Model Dev., 4 (3), 543–570, doi:{10.5194/gmd-4-543-2011}, 2011.

Jonsson, A. I., J. de Grandpré, V. I. Fomichev, J. C. McConnell, and S. R. Beagley, Doubled CO2-induced cooling in the middle atmosphere: Photochemical analysis of the ozone radiative feedback, J. Geophys. Res., 109, D24103, doi:10.1029/2004JD005093, 2004.

Josse, B., Simon, P., Peuch, V. H.: Radon global simulations with the multiscale chemistry and transport model MOCAGE, *Tellus-B*, 56, 339-356 , 2004.

Kerkweg, A., Buchholz, J., Ganzeveld, L., Pozzer, A., Tost, H., and Jöckel, P.: Technical Note: An implementation of the dry removal processes DRY DEPosition and SEDImentation

in the Modular Earth Submodel System (MESSy), Atmos. Chem. Phys., 6, 4617-4632, doi:10.5194/acp-6-4617-2006, 2006a.

Kerkweg, A., Sander, R., Tost, H., and Jöckel, P.: Technical note: Implementation of prescribed (OFFLEM), calculated (ONLEM), and pseudo-emissions (TNUDGE) of chemical species in the Modular Earth Submodel System (MESSy), Atmos. Chem. Phys., 6, 3603-3609, doi:10.5194/acp-6-3603-2006, 2006b.

Kinnison, D. E., Brasseur, G.P., S. Walters, S., Garcia, R.R., Marsh, D.R., Sassi, F., Harvey, V.L., Randall, C.E., Emmons, L., Lamarque, J.-F., Hess, P., Orlando, J.J., Tie, X.X., Randel, W., Pan, L., Gettelman, A., Granier, C., Diehl, T., Niemeier, U., Simmons, A.J.., Sensitivity of Chemical Tracers to Meteorological Parameters in the MOZART-3 Chemical Transport Model. J. Geophys. Res., 112, D20302, doi:10.1029/2006JD007879, 2007.

Kirner, O., Ruhnke, R., Buchholz-Dietsch, J., Jöckel, P., Brühl, C., and Steil, B.: Simulation of polar stratospheric clouds in the chemistry-climate-model EMAC via the submodel PSC, Geosci. Model Dev., 4, 169-82, doi:10.5194/gmd-4-169-2011, 2011.

Klinger, C., V. Eyring, M. Righi, I. Cionni, P. Jöckel, et al., Quantitative evaluation of ozone and selected climate parameters in the chemistry-climate model EMAC, GMD, in preparation, 2012.

Koch, D., Jacob, D., Tegen, I., Rind, D., and Chin, M.: Tropospheric sulfur simulation and sulfate direct radiative forcing in the Goddard Institute for Space Studies general circulation model, J. Geophys. Res., 104, 23 799–23 822, 1999.

Koch, D., G.A. Schmidt, and C.V. Field. Sulfur, sea salt and radionuclide aerosols in GISS ModelE. *J. Geophys. Res.*, **111**, D06206, doi:10.1029/2004JD005550, 2006.

Lamarque, J.-F., D. E. Kinnison, P.G. Hess and F. Vitt, Simulated lower stratospheric trends between 1970 and 2005: identifying the role of climate and composition changes. J. Geophys. Res., 113, D12301, doi:10.1029/2007JD009277, 2008.

Lamarque, J.-F., G. P. Kyle, M. Meinshausen. K. Riahi, S. J. Smith, D. P. van Vuuren, A. Conley, F. Vitt. Global and regional evolution of short-lived radiatively-active gases and aerosols in the Representative Concentration Pathways. Climatic Change, doi:10.1007/s10584-011-0155-0, 2011.

Lamarque, J.-F, L. K. Emmons, P. G. Hess, D. E. Kinnison, S. Tilmes, F. Vitt, C. L. Heald, E. A. Holland, P. H. Lauritzen, J. Neu, J. J. Orlando, P. Rasch, G. Tyndall. CAM-chem: description and evaluation of interactive atmospheric chemistry in CESM. Geosci. Mod. Dev., 5, 369-411, doi:10.5194/gmd-5-369-2012, 2012.

Lamarque, J.-F., T. C. Bond, V. Eyring, C. Granier, A. Heil, Z. Klimont, D. Lee, C. Liousse, A. Mieville, B. Owen, M. G. Schultz, D. Shindell, S. J. Smith, E. Stehfest, J. Van Aardenne, O. R. Cooper, M. Kainuma, N. Mahowald, J. R. McConnell, V. Naik, K. Riahi, and D. P. van Vuuren, Historical (1850–2000) gridded anthropogenic and biomass burning emissions of reactive gases and aerosols: methodology and application, Atmos. Chem. Phys., 10, 7017–7039, doi:10.5194/acp-10-7017-2010, 2010

Lander, J. and B. J. Hoskins, Believable scales and parameterizations in a spectral transform model, Mon. Weather Rev., 125, 292-303, 1997.

Law, K.S., and J.A. Pyle, Modelling trace gas budgets in the troposphere. 1. ozone and odd nitrogen, J.G.R. 98, pp. 18,377-18,400, 1993.

Lee, Y. H., and Adams, P. J.: A Fast and Efficient Version of the TwO-Moment Aerosol Sectional (TOMAS) Global Aerosol Microphysics Model, Aerosol Science and Technology, 46, 678-689, 10.1080/02786826.2011.643259, 2011.

Lefèvre, F., Brasseur, G. P., Folkins, I., Smith, A. K., and Simon, P.: Chemistry of the 1991–1992 stratospheric winter: threedimensional model simulations, J. Geophys. Res., 99, 8183–8195, 1994.

Liao, H., P. J. Adams, S. H. Ching, J.H Seinfeld, L.J. Mickley and D.J. Jacob., Interactions between tropospheric chemistry and aerosols in a unified general circulation model, J. Geophys. Res., 108(D1), 4001, doi:10.1029/2001JD001260, 2003.

Li, D. and K. P. Shine, A 4-Dimensional Ozone Climatology for UGAMP Models, UGAMP Internal Report No. 35, April 1995. See http://badc.nerc.ac.uk/data/ugamp-o3-climatology/ugamp_help.html

Lin, S.-J. (2004), A vertically Lagrangian finite-volume dynamical core for global models. Mon. Wea.

Lin, S. J. and R. B. Rood, 1996: Multidimensional flux-form semi-Lagrangian transport schemes. Mon. Wea. Rev., 124(9): 2046-2070.

Liu, X., R. C. Easter, S. J. Ghan, R. Zaveri, P. Rasch, X. Shi, J.-F. Lamarque, A. Gettelman, H. Morrison, F. Vitt, A. Conley, S. Park, R. Neale, C. Hannay, A. M. L. Ekman, P. Hess, N. Mahowald, W. Collins, M. J. Iacono, C. S. Bretherton, M. G. Flanner, and D. Mitchell, 2012: Toward a minimal representation of aerosols in climate models: Description and evaluation in the Community Atmosphere Model CAM5. Geosci. Model Dev., 5, 709–739, doi:10.5194/gmd-5-709-2012.

Liu, X., J. E. Penner, S. J. Ghan and M. Wang, 2007: Inclusion of ice microphysics in the NCAR community atmospheric model version 3 (CAM3). J. Climate, 20(18): 4526-4547 DOI 10.1175/Jcli4264.1.

Madec, G., Delecluse, P., Imbard, I. and Levy, C. (1999): OPA 8.1 Ocean General Circulation Model reference manual. Note du Pôle de modélisation No. 11, Inst. Pierre-Simon Laplace (IPSL), France, 91pp.

Lohmann, U. and Roeckner, E.: Design and performance of a new cloud microphysics scheme developed for the ECHAM general circulation model, Clim. Dynam., 12, 557-572, 1996.

Madronich, S., and Flocke, S.: The role of solar radiation in atmospheric chemistry, Handbook of Environmental Chemistry, P. Boule, ed., Springer-Verland, Heidelberg, pp 1-26, 1998.

Mahowald, N., D. R. Muhs, S. Levis, P. J Rasch, M. Yoshioka, C. S. Zender and C. Luo, Change in atmospheric mineral aerosols in response to climate: last glacial period, pre-industrial, modern and doubled-carbon dioxide climates, J. Geophys. Res., 111, D10202, doi:10210.11029/12005JD006653, 2006a.
Mahowald, N., J.-F. Lamarque, X. X. Tie and E. Wolff, Sea salt aerosol response to climate change: last glacial maximum, pre-industrial, and doubled-carbon dioxide climates, J. Geophys. Res., 111, D05303, doi:10.1029/2005JD006459, 2006b.

Manzini, E., M. A. Giorgetta, M. Esch, L. Kornblueh, and E. Roeckner, 2006: The influence of sea surface temperatures on the northern winter stratosphere: Ensemble simulations with the MAECHAM5 model. J. Climate, 19, 3863–3881.

Mari, C., Jacob, D. J., and Bechtold, P.: Transport and scavenging of soluble gases in a deep convective cloud, J. Geophys. Res., 105, 22 255–22 267, 2000.

Martin, G. M.; Bellouin, N.; Collins, W. J.; Culverwell, I. D.; Halloran, P. R.; Hardiman, S. C.; Hinton, T. J.; Jones, C. D.; McDonald, R. E.; McLaren, A. J.; O'Connor, F. M.; Roberts, M. J.; Rodriguez, J. M.; Woodward, S.; Best, M. J.; Brooks, M. E.; Brown, A. R.; Butchart, N.; Dearden, C.; Derbyshire, S. H.; Dharssi, I.; Doutriaux-Boucher, M.; Edwards, J. M.; Falloon, P. D.; Gedney, N.; Gray, L. J.; Hewitt, H. T.; Hobson, M.; Huddleston, M. R.; Hughes, J.; Ineson, S.; Ingram, W. J.; James, P. M.; Johns, T. C.; Johnson, C. E.; Jones, A.; Jones, C. P.; Joshi, M. M.; Keen, A. B.; Liddicoat, S.; Lock, A. P.; Maidens, A. V.; Manners, J. C.; Milton, S. F.; Rae, J. G. L.; Ridley, J. K.; Sellar, A.; Senior, C. A.; Totterdell, I. J.; Verhoef, A.; Vidale, P. L.; Wiltshire, A., 2011: The HadGEM2 family of Met Office Unified Model climate configurations. Geosci. Model Dev., 4, 723-757, http://dx.doi.org/10.5194/gmd-4-723-2011

Meehl, G.A., and Coauthors (2012), Climate System Response to External Forcings and Climate Change Projections in CCSM4. J. Climate, 25, 3661–3683. doi: http://dx.doi.org/10.1175/JCLI-D-11-00240.1

Meehl, G.A., T.F. Stocker, W.D. Collins, P. Friedlingstein, A.T. Gaye, J.M. Gregory, A. Kitoh, R. Knutti, J.M. Murphy, A. Noda, S.C.B. Raper, I.G. Watterson, A.J. Weaver and Z.-C. Zhao, 2007: Global Climate Projections. In: Climate Change 2007: The Physical Science Basis. Contribution of Working Group I to the Fourth Assessment Report of the Intergovernmental Panel on Climate Change [Solomon, S., D. Qin, M. Manning, Z. Chen, M. Marquis, K.B. Averyt, M. Tignor and H.L. Miller (eds.)]. Cambridge University Press, Cambridge, United Kingdom and New York, NY, USA.

Meinshausen, M., S. J. Smith, K. Calvin, J. S. Daniel, M. L. T. Kainuma, J-F. Lamarque, K. Matsumoto, S. Montzka, S. Raper, K. Riahi, A. Thomson, G. J. M. Velders, D.P. van Vuuren, The RCP Greenhouse Gas Concentrations and their Extensions from 1765 to 2300. Climatic Change, 109, 213-241,DOI 10.1007/s10584-011-0156-z, 2011.

Metzger, S., F. Dentener, S. Pandis, and J. Lelieveld, Gas/aerosol partitioning: 1. A computationally efficient model, J. Geophys. Res., 107, D16, doi:10.1029/2001JD001102, 2002.

Molod, A., L. Takacs, M. Suarez, J. Bacmeister, I.-S. Song, and A. Eichmann (2012). The GEOS-5 Atmospheric General Circulation Model: Mean Climate and Development from

MERRA to Fortuna. Technical Report Series on Global Modeling and Data Assimilation, 28.

Moorthi, S., and M.J. Suarez (1992), Relaxed Arakawa-Schubert, A Parameterization of Moist Convection for General-Circulation Models. Mon. Wea. Rev., 120, 978-1002.

Morrison, H. and A. Gettelman, 2008: A new two-moment bulk stratiform cloud microphysics scheme in the community atmosphere model, version 3 (CAM3). Part I: Description and numerical tests. J. Climate, 21(15): 3642-3659 DOI Doi 10.1175/2008jcli2105.1.

Myhre, G., Bellouin, N., Berglen, T. F., Berntsen, T. K., Boucher, O. Grini A., S. A. Iaksen I.S.A. , Johnstrud, M. , Mishchenk M.I., Stordal, F.and Tanré, D.7 .: Comparison of the radiative properties and direct radiative effect of aerosols from a global aerosol model and remote sensing data over ocean, Tellus Series B-Chemical And Physical Meteorology, 59(1), 115-129, 2007.

Myhre, G., Berglen, T. F., Johnsrud, M., Hoyle, C. R., Berntsen, T. K., Christopher, S. A.; Fahey, D. W.; Isaksen, I. S. A.; Jones, T. A.; Kahn, R. A.; Loeb, N.; Quinn, P.; Remer, L.; Schwarz, J. P.; Yttri, K. E..: Modelled radiative forcing of the direct aerosol effect with multi-observation evaluation, Atmospheric Chemistry and Physics, 9(4), 1365-1392, 2009.

Myhre, G., Grini, A. and Metzger, S.: Modelling of nitrate and ammonium-containing aerosols in presence of sea salt, Atmospheric Chemistry and Physics, 6, 4809-4821, 2006.

Naik, V., Horowitz, L. W., Fiore, A. M., Ginoux, P., Mao, J., Aghedo, A., and Levy II, H.: Preindustrial to present day impact of changes in short-lived pollutant emissions on atmospheric composition and climate forcing, submitted to J. Geophys. Res., June 2012.

Nightingale, P. D., Malin, G., Law, C. S., Watson, A. J., Liss, P. S., Liddicoat M.I., Boutin J. and Upstill-Goddard R.C. : In situ evaluation of air-sea gas exchange parameterizations using novel conservative and volatile tracers, Global Biogeochem. Cy, 14(1), 373-387, 2000.

Nordeng, T. E.: Extended versions of the convective parametrization scheme at ECMWF and their impact on the mean and transient activity of the model in the tropics, Tech. rep., ECWMF, 1994.

O'Connor, F., C. Johnson, O. Morgenstern, M. Sanderson, P. Young, W. Collins, and J. Pyle, Evaluation of the new UKCA climate-composition model. Part II. The troposphere, Geosci. Model Dev. (2011), submitted.

Oman, L.D., J. R. Ziemke, A. R. Douglass, D.W. Waugh, C. Lang, J.M. Rodriguez, and J.E. Nielsen (2011), The response of tropical tropospheric ozone to ENSO, Geophys. Res. Lett., 38, L13706, doi:10.1029/2011GL047865.

Pacifico, F., G.A. Folberth, C.D. Jones, S.P. Harrison, and W.J. Collins, Sensitivity of biogenic isoprene emissions to past, present and future environmental conditions and implications for atmospheric chemistry, J.G.R, submitted.

Park, S. and C. S. Bretherton, 2009: The University of Washington Shallow convection and moist turbulence schemes and their impact on climate simulations with the community atmosphere model. J. Climate, 22(12): 3449-3469 DOI Doi 10.1175/2008jcli2557.1.

Park, S., C. Bretherton and P. J. Rasch, 2011: Global cloud simulation in the CAM5, in preparation.

Penner, J. E., Atherton, C. S., Dignon, J., Ghan, S. J., Walton, J. J., and Hameed, S.: Global emissions and models of photochemically active compounds, in Global Atmospheric Biospheric Chemistry, edited by R. G. Prinn, 223–247, Plenum, New York, 1994.

Pope, V. D., M. L. Gallani, P. R. Rowntree, and R. A. Stratton, 2000: The impact of new physical parametrizations in the Hadley Centre climate model: HadAM3. Clim. Dynam., 16, 123–146, doi:10.1007/s003820050009.

Pozzer, A., Jöckel, P., Sander, R., Williams, J., Ganzeveld, L., and Lelieveld, J.: Technical Note: The MESSy-submodel AIRSEA calculating the air-sea exchange of chemical species, Atmos. Chem. Phys., 6, 5435-5444, doi:10.5194/acp-6-5435-2006, 2006.

Prather, M. J.: Numerical Advection By Conservation Of 2nd-Order Moments, Journal of Geophysical Research-Atmospheres, 91(D6), 6671-6681, 1986.

Price, C., and D. Rind (1992), A Simple Lightning Parameterization for Calculating Global Lightning Distributions, J. Geophys. Res., 97(D9), 9919–9933, oi:10.1029/92JD00719.

Price, C. and D. Rind, Modelling global lightning distributions in a general circulation model, M. Weather Rev., 122, pp. 1930-1939, doi:10.1175/1520-0493.

Price, C., J. Penner, and M. Prather (1997), NOx from lightning 1. Global distribution based on lightning physics, J. Geophys. Res., 102(D5), 5929–5941, doi:10.1029/96JD03504.

Prinn, R. G., Weiss, R. F., Fraser, P. J., Simmonds, P. G., Cunnold, D. M., Alyea, F. N., O'Doherty, S., Salameh, P., Miller, B. R., Huang, J., Wang, R. H. J., Hartley, D. E., Harth, C., Steele, L. P., Sturrock, G., Midgley, P. M., and McCulloch, A.: A history of chemically and radiatively important gases in air deduced from ALE/GAGE/AGAGE, J. Geophys. Res., 105, 17 751–17 792, 2000.

Putman, W. M., and Lin, S.-J.: Finite-volume transport on various cubed-sphere grid, J. Comput. Phys., 227, 55-78, 2007.

Reynolds, R.W., N.A. Rayner, T.M. Smith, D.C. Stokes and W. Wang (2002), An improved in situ and satellite SST analysis for climate. J. Clim., 15, 1609-1625.

Rienecker, M.M., M.J. Suarez, R. Todling, J. Bacmeister, L. Takacs, H.-C. Liu, W. Gu, M. Sienkiewicz, R.D. Koster, R. Gelaro, I. Stajner, and J.E. Nielsen (2008), The GEOS-5 Data Assimilation System - Documentation of Versions 5.0.1, 5.1.0, and 5.2.0. Technical Report Series on Global Modeling and Data Assimilation, 27.

Roeckner, E., Brokopf, R., Esch, M., Giorgetta, M., Hagemann, S., Kornblueh, L., Manzini, E., Schlese, U., and Schulzweida,U.: Sensitivity of simulated climate to horizontal and vertical resolution in the ECHAM5 atmosphere model, J. Climate, 19, 3771–3791, 2006.

Rotman, D. A., C. S. Atherton, D. J. Bergmann, P. J. Cameron-Smith, C. C. Chuang, P. S. Connell, J. E. Dignon, A. Franz, K. E. Grant, D. E. Kinnison, C. R. Molenkamp, D. D. Proctor, J. R. Tannahill, IMPACT, the LLNL 3-D global atmospheric chemical transport model for the combined troposphere and stratosphere: Model description and analysis of ozone and other trace gases, J. Geophys. Res., 109(D4), D04303., 2004.

Sander, R., Kerkweg, A., Jöckel, P., and Lelieveld, J.: Technical note: The new comprehensive atmospheric chemistry module MECCA, Atmos. Chem. Phys., 5, 445-450, 2005.

Sanderson, M. G., C. D. Jones, W. J. Collins, C. E. Johnson, and R. G. Derwent (2003), Effect of Climate Change on Isoprene Emissions and Surface Ozone Levels, Geophys. Res. Lett., 30(18), 1936, doi:10.1029/2003GL017642.

Sander, S. P., R.R. Friedl, D.M. Golden, M.J. Kurylo, G.K. Moortgat, H. Keller-Rudek, P.H. Wine, A.R. Ravishankara, C.E. Kolb, M.J. Molina, B.J. Finlayson-Pitts, R.E. Huie, V.L. Orkin : Chemical Kinetics and Photochemical Data for Use in Atmospheric Studies, Evaluation Number 15, JPL Publication 06-2, Jet Propulsion Laboratory, Pasadena, CA, 2006.

Sander, S. P., Friedl, R. R., Golden, D. M., Kurylo, M. J., Moortgat, G. K., Keller-Rudek, H., Wine, P. H., Ravishankara, A. R., Kolb, C. E., Molina, M. J., Finlayson-Pitts, B. J., Huie, R. E., and Orkin, V. L.: Chemical kinetics and photochemical data for use in atmospheric studies, Evaluation No. 15, JPL Publications 06-2, Jet Propulsion Laboratory, Pasadena, CA, USA, 2006.

Sato, M., J. E. Hansen, M. P. McCormick, and J. B. Pollack (1993), Stratospheric Aerosol Optical Depths, 1850–1990, J. Geophys. Res., 98(D12), 22,987–22,994, doi:10.1029/93JD02553.

Schultz, M. and Rast, S.: Emission datasets and methodologies for estimating emissions, available at: http://retro.enes.org, last access: 16 February 2010, RETRO Report D1-6, 2007.

Scinocca, J. F., N. A. McFarlane, M. Lazare, J. Li and D. Plummer, Technical Note: The CCCma third generation AGCM and its extension into the middle atmosphere, Atmos. Chem. Phys., 8, 7055–7074, doi:10.5194/acp-8-7055-2008, 2008.

Sekiguchi, M. and Nakajima, T. (2008), A k-distribution based radiation code and its computational optimization for an atmospheric general circulation model, J. Quant. Spectrosc. Radiat. Transfer, 109, 2779–2793, doi:10.1016/j.jqsrt.2008.07.013.

Shindell, D. T., G. Faluvegi, N. Unger, E. Aguilar, G. A. Schmidt, D. Koch, S. E. Bauer, and R. L. Miller (2006), Simulations of preindustrial, present-day, and 2100 conditions in the NASA GISS composition and climate model G-PUCCINI, Atmos. Chem. Phys., 6, 4427-4459.

Shindell, D. T., Grenfell, J. L., Rind, D., Price, C., and Grewe, V.: Chemistry climate interactions in the Goddard Institute for Space Studies general circulation model 1. Tropospheric chemistry model description and evaluation, J. Geophys. Res., 106, 8047–8076, 2001.

Skeie, R. B., Berntsen, T., Myhre, G., Pedersen, C. A., Strom, J., S. Gerland, and J. A. Ogren.: Black carbon in the atmosphere and snow, from pre-industrial times until present, Atmospheric Chemistry and Physics, 11(14), 6809-6836, 2011a.

Skeie, R. B., Berntsen, T. K., Myhre, G., Tanaka, K., Kvalevag, M. M. and C. R. Hoyle: Anthropogenic radiative forcing time series from pre-industrial times until 2010, Atmospheric Chemistry and Physics, 11(22), 11827-11857, 2011b.

Spiro, P. A., Jacob, D. J., and Logan, J. A.: Global Inventory of Sulfur Emissions With 1°×1°_Resolution, J. Geophys. Res., 97, 6023-6036, 1992.

Stamnes, K., Tsay, S. C., Wiscombe, W. and Jayaweera, K.: Numerically Stable Algorithm For Discrete-Ordinate-Method Radiative-Transfer In Multiple-Scattering And Emitting Layered Media, Applied Optics, 27(12), 2502-2509, 1988.

Stevenson, D., Johnson, C., Highwood, E., Gauci, V., Collins, W., and Derwent, R.: Atmospheric impact of the 1783-1784 Laki eruption : Part I chemistry modelling, Atmos. Chem. Phys. Discuss., 3, 551–596, 2003.

Stevenson, D. S., Johnson, C. E., Collins, W. J., and Derwent, R. G.: Intercomparison and evaluation of atmospheric transport in a Lagrangian model (STOCHEM) and an Eulerian model (UM) using 222Rn as a short-lived tracer, Q. J. R. Meteorol. Soc., 124, 2477–2491, 1998

Stevenson, D. S., R. M. Doherty, M. G. Sanderson, W. J. Collins, C. E. Johnson, and R. G. Derwent (2004), Radiative forcing from aircraft NOx emissions: Mechanisms and seasonal dependence, J. Geophys. Res., 109, D17307, doi:10.1029/2004JD004759.

Stockwell, W. R., Kirchner, F., Khun, M., and Seefeld, S.: A new mechanism for regional atmospheric chemistry modelling, J. Geophys. Res., 102, 25 847–25 879, 1997.

Strahan, S.E., B.N. Duncan , and P. Hoor (2007), Observationally derived transport diagnostics for the lowermost stratosphere and their application to the GMI chemistry and transport model, Atmos. Chem. Phys., 7, 2435-2445.

Stratospheric Processes and Their Role in Climate (SPARC), Assessment of Stratospheric Aerosol Properties (ASAP), Tech. Rep. WMO-TD 1295, WCRP Ser. Rep. 124, SPARC Rep. 4, World Clim. Res. Programme, Geneva, Switzerland, 2006.

Sudo, K., and H. Akimoto (2007), Global source attribution of tropospheric ozone: Long-range transport from various source regions, J. Geophys. Res., 112, D12302, doi:10.1029/2006JD007992.

Sudo, K., M. Takahashi, J. Kurokawa, and H. Akimoto (2002), CHASER: A globalchemical model of the troposphere 1. Model description, J. Geophys. Res., 107, 4339, doi:10.1029/2001JD001113.

Takemura, T., H. Okamoto, Y. Maruyama, A. Numaguti, A. Higurashi, and T. Nakajima (2000), Global three-dimensional simulation of aerosol optical thickness distribution of various origins, J. Geophys. Res., 105(D14), 17,853–17,873, doi:10.1029/2000JD900265.

Takemura, T., Nakajima, T., Dubovik, O., Holben, B. N., and Kinne, S. (2002), Single-scattering albedo and radiative forcing of various aerosol species with a global three-dimensional model, J. Climate, 15, 333–352, doi:10.1175/1520-0442(2002)0152.0.CO

Takemura, T., T. Nozawa, S. Emori, T. Y. Nakajima, and T. Nakajima (2005), Simulation of climate response to aerosol direct and indirect effects with aerosol transport-radiation model, J. Geophys. Res., 110, D02202, doi:10.1029/2004JD005029.

Tanre, D., Geleyn, J.-F., and Slingo, J. M.: First results of the introduction of an advanced aerosol-radiation interaction in the ECMWF low resolution global model, in: Aerosols and their climatic effects, edited by: Gerber, H. and Deepak, A., pp. 133–177, A. Deepak, Hampton, VA, 1984.

Task Force on Hemispheric Transport of Air Pollution (TF-HTAP): Hemispheric Transport of Air Pollution 2010, Air Pollut. Stud. 17, edited by: Dentener, F., Keating, T., and Akimoto, H., UNECE, Geneva, Switzerland, available at: http://www.htap.org/, 2010.

Teyssèdre, H., Michou, M., Clark, H. L., Josse, B., Karcher, F., Olivié, D., Peuch, V.-H., Saint-Martin, D., Cariolle, D., Attié, J.-L., Nédélec, P., Ricaud, P., Thouret, V., van der A, R. J., Volz-Thomas, A., and Chéroux, F.: A new tropospheric and stratospheric Chemistry and Transport Model MOCAGE-Climat for multi-year studies: evaluation of the present-day climatology and sensitivity to surface processes, *Atmos. Chem. Phys.*, 7, 5815-5860, doi:10.5194/acp-7-5815-2007, 2007.

Tiedtke, M.: A Comprehensive Mass Flux Scheme For Cumulus Parameterization In Large-Scale Models, Monthly Weather Review, 117(8), 1779-1800, 1989.

Tie, X.X., G. P. Brasseur, L. K. Emmons, L. Horowitz, and D. Kinnison : Effects of aerosols on tropospheric oxidants: A global model study, J. Geophys. Res., 106, 2931– 2964, 2001.

Tie, X.X., S. Madronich, S. Walters, R. Zhang, P. Rasch, and W. Collins, Assessment of the global impact of aerosols on tropospheric oxidants, J. Geophys. Res., 110, doi:10.1029/2004JD005359, 2005.

Tost, H., Jöckel, P., Kerkweg, A., Sander, R., and Lelieveld, J.: Technical note: A new comprehensive SCAVenging submodel for global atmospheric chemistry modelling, Atmos. Chem. Phys., 6, 565–574, 2006a.

Tost, H., Jöckel, P., and Lelieveld, J.: Influence of different convection parameterisations in a GCM, Atmos. Chem. Phys. 6, 5475–5493, 2006b.

Valcke, S. (2006): OASIS3 User Guide (prism_2-5), PRISM Report No 2, 6th Ed., CERFACS, Tolouse, France, 64 pp.

Voldoire, A. E. Sanchez-Gomez, D. Salas y Mélia, B. Decharme, C. Cassou, S.Sénési, S. Valcke, I. Beau, A. Alias, M. Chevallier, M. Déqué, J. Deshayes, H. Douville, E. Fernandez, G. Madec, E. Maisonnave , M.-P. Moine, S. Planton, D. Saint-Martin, S. Szopa, S. Tyteca, R. Alkama, S. Belamari, A. Braun, L. Coquart, F. Chauvin., 2012, The CNRM-CM5.1 global climate model : description and basic evaluation , Clim. Dyn., DOI:10.1007/s00382-011-1259-y

Wang, Y., D.J. Jacob, and J.A. Logan (1998), Global simulation of tropospheric O3 -NOx - hydrocarbon chemistry: 1. Model formulation, J. Geophys. Res., 103, 10 713–10 725.

Watanabe, S., Hajima, T., Sudo, K., Nagashima, T., Takemura, T., Okajima, H., Nozawa, T., Kawase, H., Abe, M., Yokohata, T., Ise, T., Sato, H., Kato, E., Takata, K., Emori, S., and Kawamiya, M. (2011), MIROC-ESM 2010: model description and basic results of CMIP5-20c3m experiments, Geosci. Model Dev., 4, 845–872, doi:10.5194/gmd-4-845-2011.

Wesely, M.L., Parameterization of surface resistances to gaseous dry deposition in regional-scale numerical models, Atmos. Environ., 23, 6, pp. 1293-1304, 1989.

Wild, O., X. Zhu, and M. Prather (2000), Fast-J: Accurate simulation of in- and below-cloud photolysis in tropospheric chemical models, J. Atmos. Chem. 37, 245-282.

Yienger, J.J. and H.Levy II (1995), Empirical model of global soil-biogenic NOx emissions, J. Geophys. Res., 100(D6), 11447-11464.

Young, P.J., A. Arneth, G. Schurgers, G. Zeng, J. A. Pyle, The CO2 inhibition of terrestrial isoprene emission significantly affects future ozone projections. Atmospheric Chemistry and Physics 9, pp. 2,793–2,803.

Zhang, G. J. and N. A. McFarlane, 1995: Sensitivity of climate simulations to the parameterization of cumulus convection in the Canadian Climate Center general circulation model. Atmosphere-Ocean 33(3): 407-446

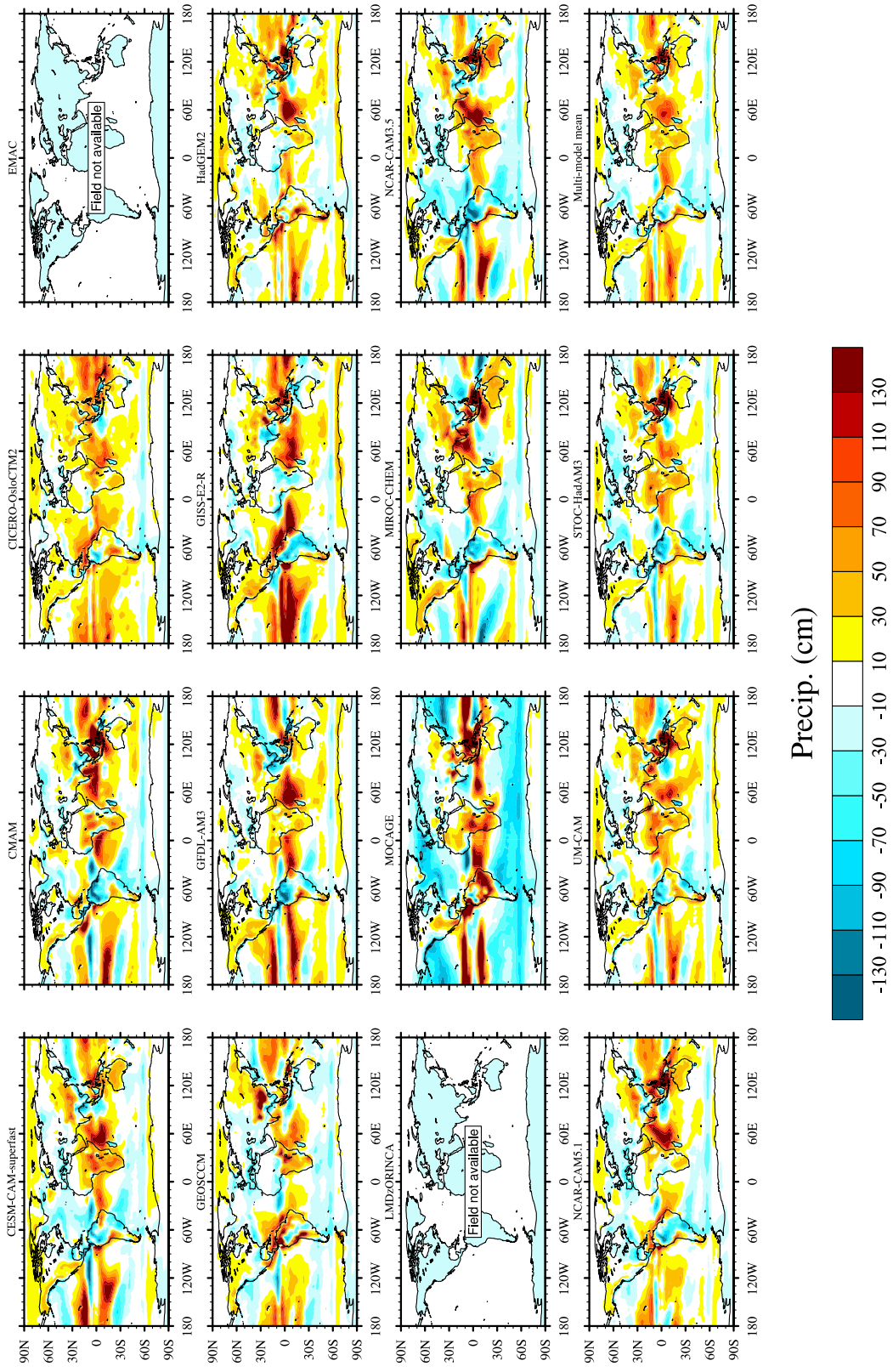

Figure S1. Difference (model-obs) for annual mean precip (against GPCP)

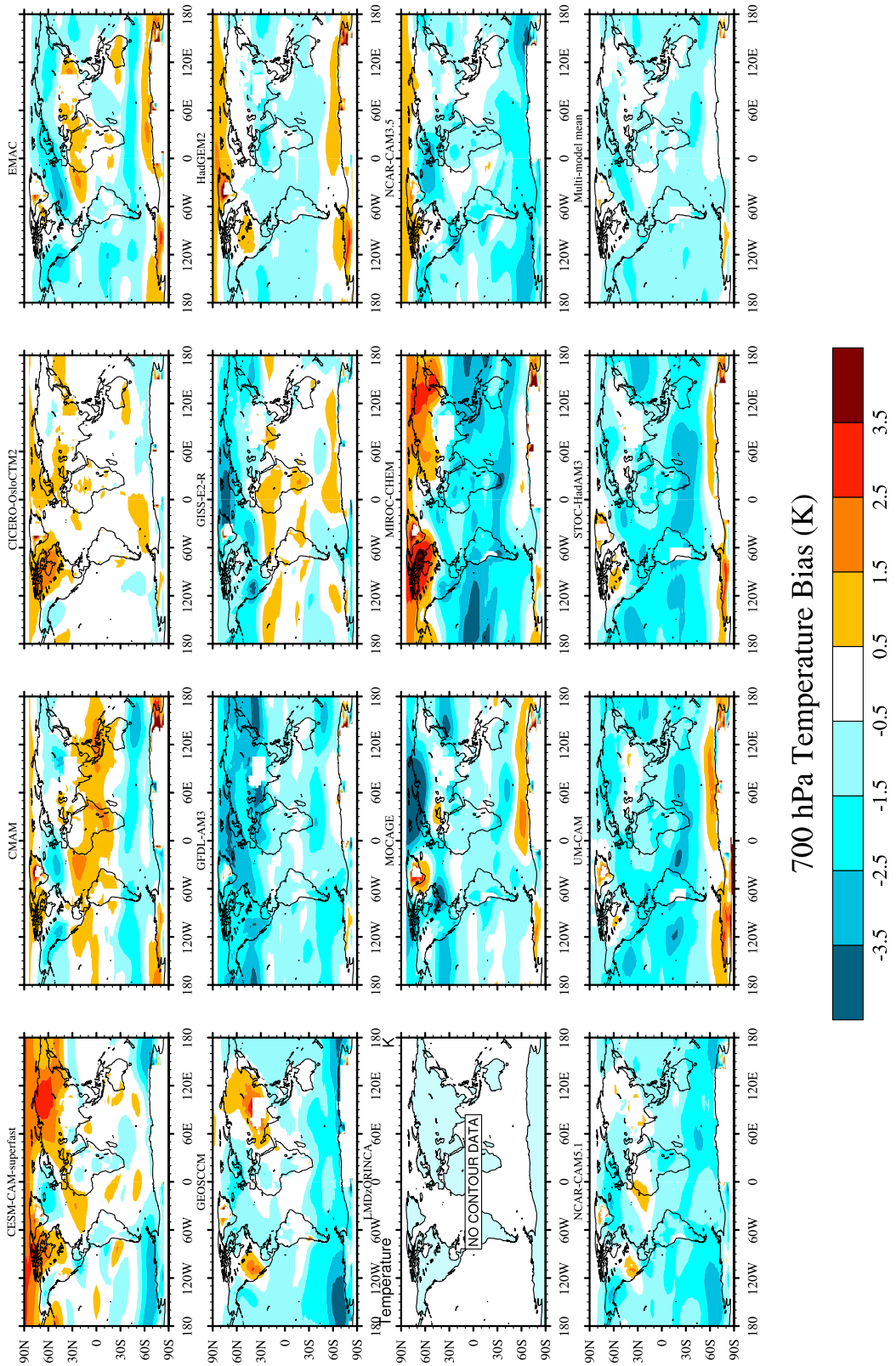

Figure S2. Same as Fig. S1 but for 700 hPa temperature.

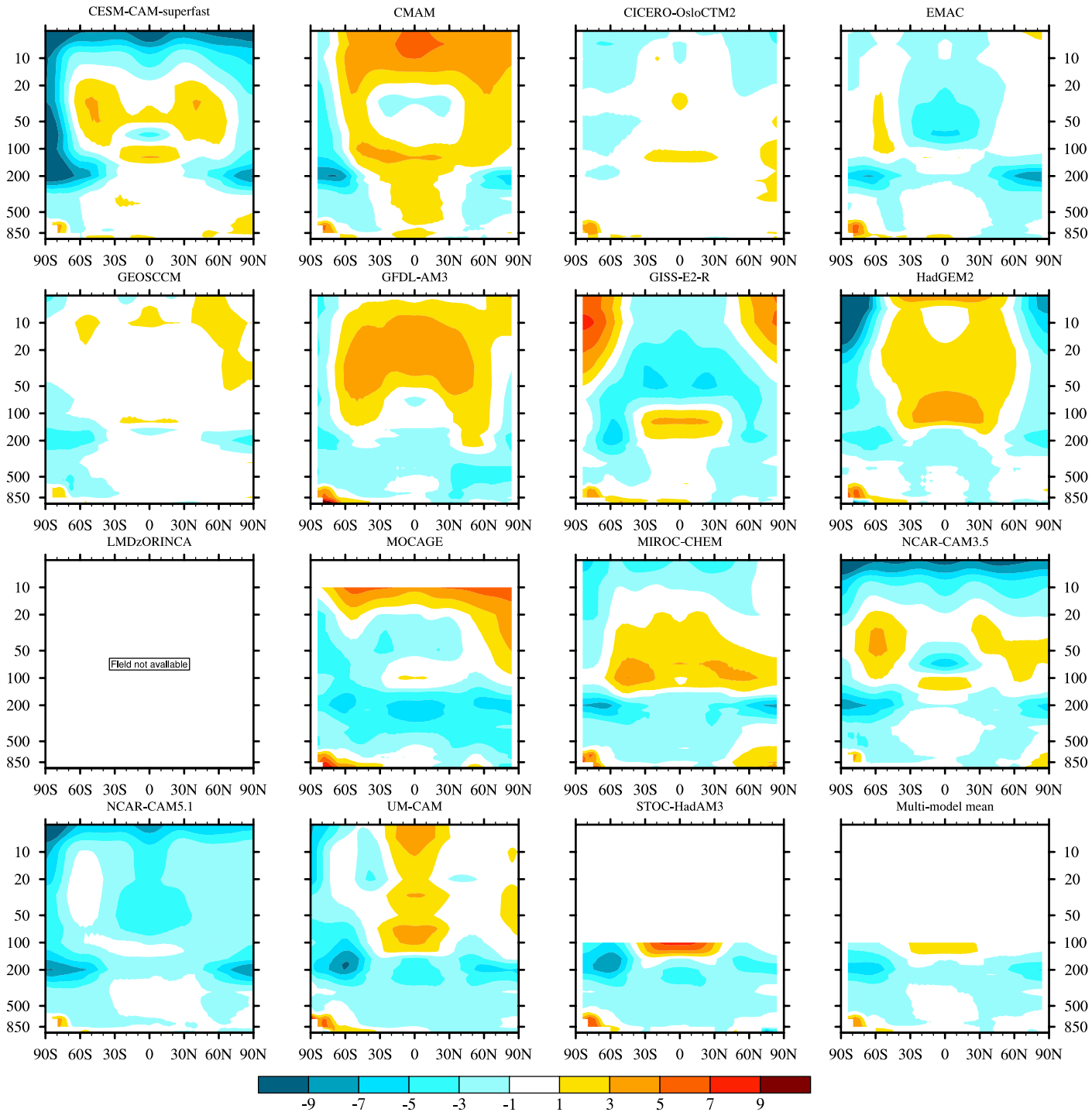

Figure S3. Zonal-annual mean T minus ERA-Interim (K).

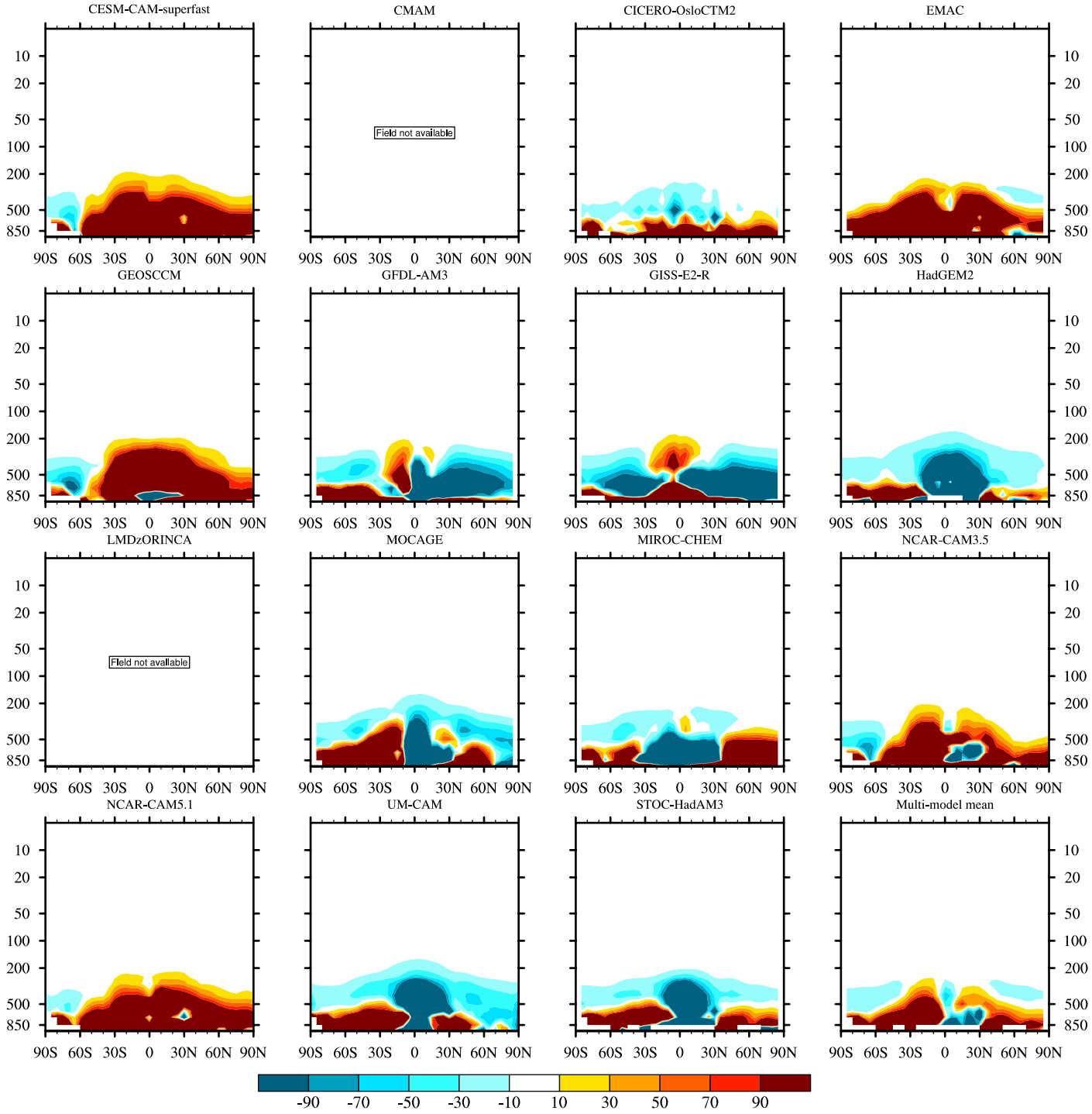

Figure S4. Zonal-annual mean Q minus ERA-Interim (10^{-6} kg/kg).

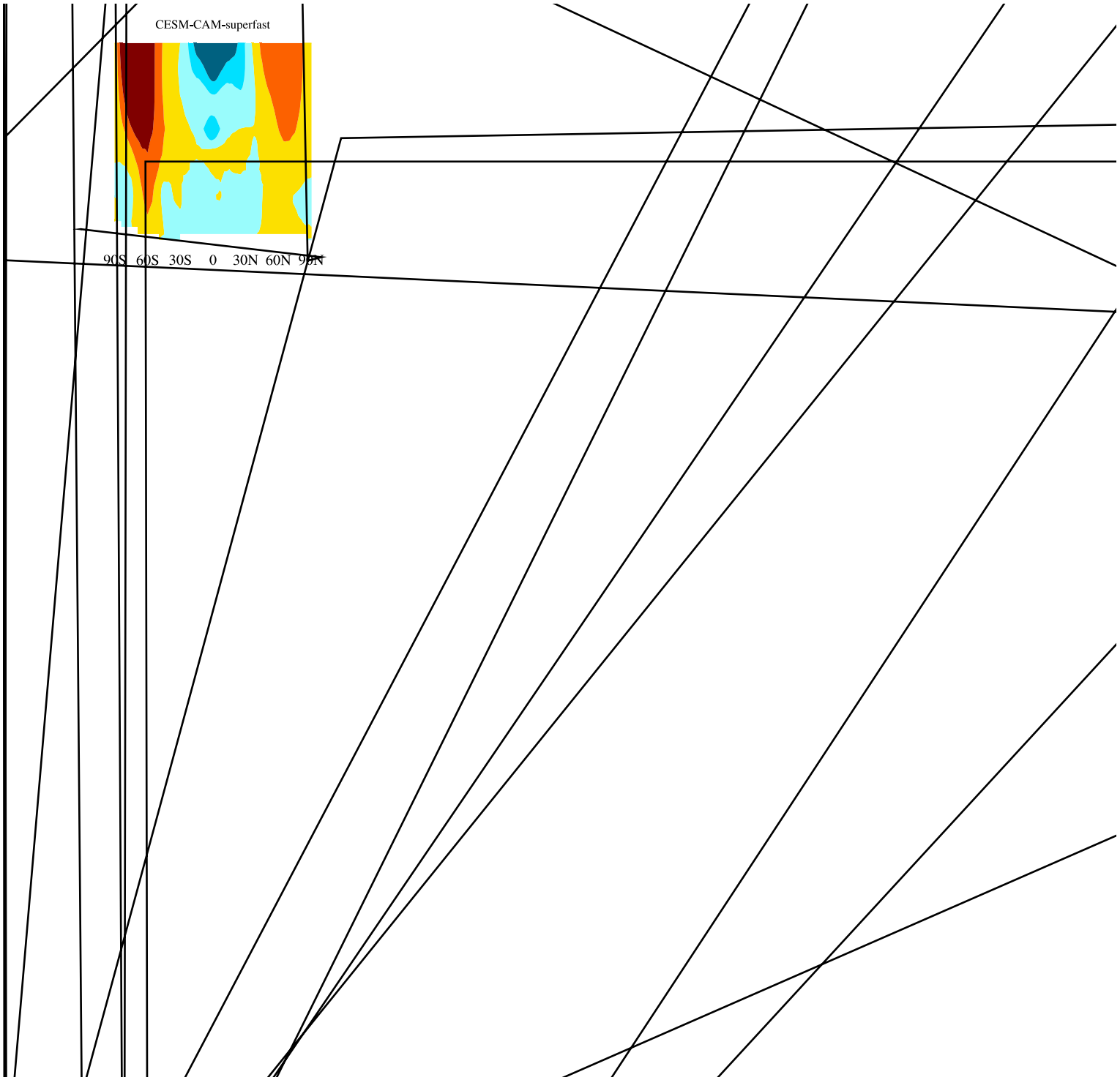

Figure S5. Zonal-annual mean U minus ERA-Interim (m/s).

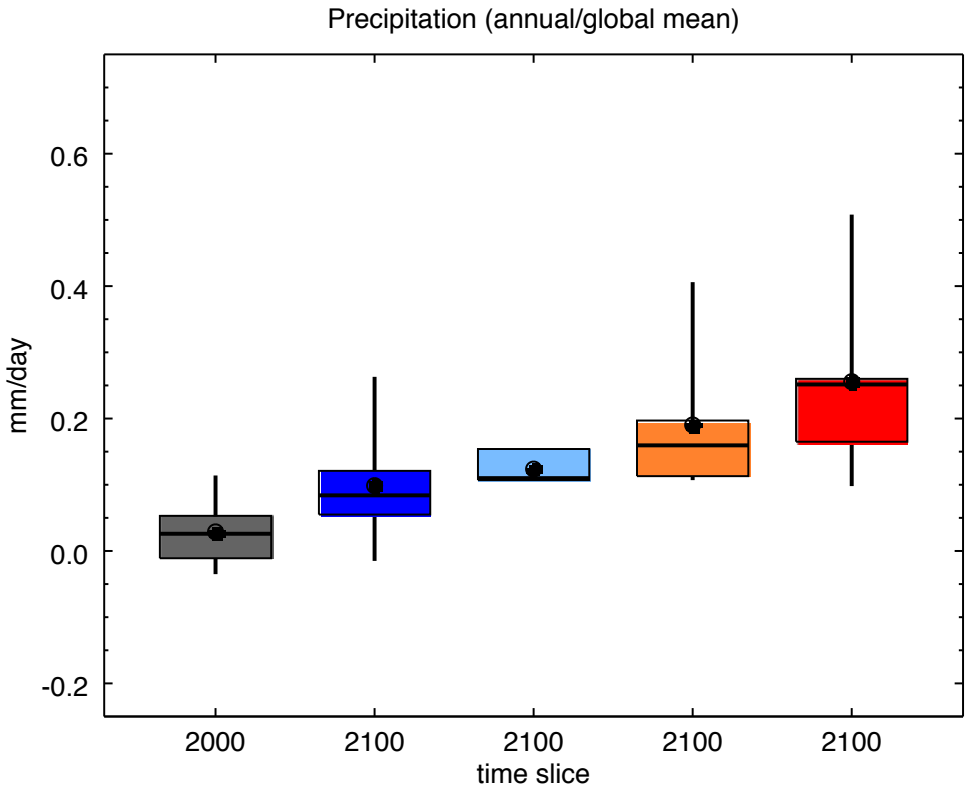

Figure S6. Same as Figure 8 with using only the models that have provided data for all timeslices: GFDL-AM3, GISS-E2Rs, MOCAGE, MIROC-CHEM and NCAR-CAM3.5.

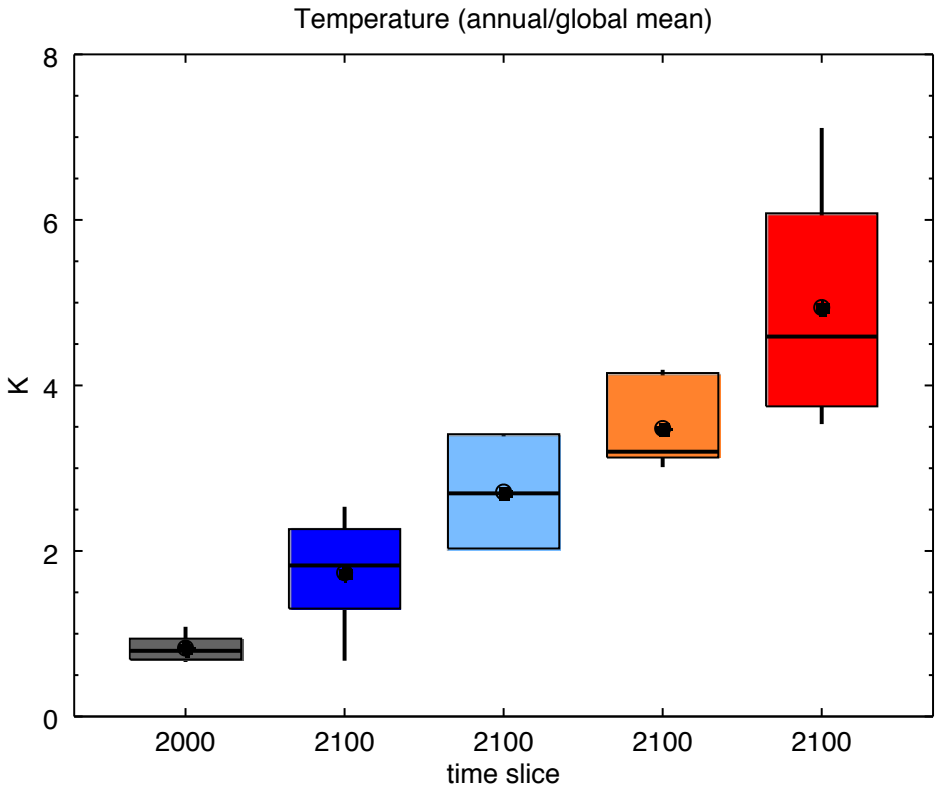

Figure S7. Same as Figure 9 with using only the models that have provided data for all timeslices: GFDL-AM3, GISS-E2Rs, MOCAGE, MIROC-CHEM and NCAR-CAM3.5.

monthly mean thermodynamics variables	file name	units
precipitation_amount	precip	kg m-2
surface_air_pressure	ps	Pa
monthly mean surface dry deposition flux, positive: down		
tendency_of_atmosphere_mass_content_of_ozone_due_to_dry_deposition	dry_o3	kg m-2 s-1
tendency_of_atmosphere_mass_content_of_nitric_acid_due_to_dry_deposition	dry_hno3	kg m-2 s-1
tendency_of_atmosphere_mass_content_of_nitrogen_dioxide_due_to_dry_deposition	dry_no2	kg m-2 s-1
surface_dry_deposition_mass_flux_of_all_nitrogen_oxides_as_nitrogen	dry_noy	kg m-2 s-1
tendency_of_atmosphere_mass_content_of_ammonia_due_to_dry_deposition	dry_nh3	kg m-2 s-1
surface_dry_deposition_mass_flux_of_ammonium_as_ammonium	dry_nh4	kg m-2 s-1
tendency_of_atmosphere_mass_content_of_sulfur_dioxide_due_to_dry_deposition	dry_so2	kg m-2 s-1
surface_dry_deposition_mass_flux_of_sulfate_as_sulfate_dry_aerosol	dry_so4	kg m-2 s-1
tendency_of_atmosphere_mass_content_of_black_carbon_dry_aerosol_due_to_dry_deposition	dry_bc	kg m-2 s-1
tendency_of_atmosphere_mass_content_of_particulate_organic_matter_dry_aerosol_due_to_dry_deposition	dry_pom	kg m-2 s-1
tendency_of_atmosphere_mass_content_of_seasalt_dry_aerosol_due_to_dry_deposition	dry_ss	kg m-2 s-1
tendency_of_atmosphere_mass_content_of_dust_dry_aerosol_due_to_dry_deposition	dry_du	kg m-2 s-1
tendency_of_atmosphere_mass_content_of_dimethyl_sulfide_due_to_dry_deposition	dry_dms	kg m-2 s-1
monthly mean stomatal flux, positive: down		
tendency_of_atmosphere_mass_content_of_ozone_due_to_dry_deposition_into_stomata	sto_o3	kg m-2 s-1
monthly mean wet deposition flux at the surface, positive: down		
surface_wet_deposition_mass_flux_of_all_nitrogen_oxides_as_nitrogen	wet_noy	kg m-2 s-1
tendency_of_atmosphere_mass_content_of_nitric_acid_due_to_wet_deposition	wet_hno3	kg m-2 s-1
tendency_of_atmosphere_mass_content_of_ammonia_due_to_wet_deposition	wet_nh3	kg m-2 s-1
surface_wet_deposition_mass_flux_of_ammonium_as_ammonium	wet_nh4	kg m-2 s-1
tendency_of_atmosphere_mass_content_of_sulfur_dioxide_due_to_wet_deposition	wet_so2	kg m-2 s-1
surface_wet_deposition_mass_flux_of_sulfate_as_sulfate_dry_aerosol	wet_so4	kg m-2 s-1
tendency_of_atmosphere_mass_content_of_black_carbon_dry_aerosol_due_to_wet_deposition	wet_bc	kg m-2 s-1
tendency_of_atmosphere_mass_content_of_particulate_organic_matter_dry_aerosol_due_to_wet_deposition	wet_pom	kg m-2 s-1
tendency_of_atmosphere_mass_content_of_seasalt_dry_aerosol_due_to_wet_deposition	wet_ss	kg m-2 s-1
tendency_of_atmosphere_mass_content_of_dust_dry_aerosol_due_to_wet_deposition	wet_du	kg m-2 s-1
tendency_of_atmosphere_mass_content_of_dimethyl_sulfide_due_to_wet_deposition	wet_dms	kg m-2 s-1

monthly mean total emission flux, positive: up, integrate 3D emission field vertically to 2d field		
tendency_of_atmosphere_mass_content_of_nox_expressed_as_nitrogen_due_to_emission	emi_nox	kg m-2 s-1
tendency_of_atmosphere_mass_content_of_carbon_monoxide_due_to_emission	emi_co	kg m-2 s-1
atmosphere_emission_mass_flux_of_non_methane_volatile_organic_compounds_as_carbon	emi_voc	kg m-2 s-1
atmosphere_emission_mass_flux_of_biogenic_non_methane_volatile_organic_compounds_as_carbon	emi_bvoc	kg m-2 s-1
tendency_of_atmosphere_mass_content_of_ammonia_due_to_emission	emi_nh3	kg m-2 s-1
tendency_of_atmosphere_mass_content_of_sulfur_dioxide_due_to_emission	emi_so2	kg m-2 s-1
atmosphere_emission_mass_flux_of_sulfate_as_sulfate_dry_aerosol	emi_so4	kg m-2 s-1
tendency_of_atmosphere_mass_content_of_black_carbon_dry_aerosol_due_to_emission	emi_bc	kg m-2 s-1
tendency_of_atmosphere_mass_content_of_primary_particulate_organic_matter_dry_aerosol_due_to_emission	emi_pom	kg m-2 s-1
atmosphere_emission_mass_flux_of_secondary_organic_matter_as_secondary_organic_matter_dry_aerosol	emi_soa	kg m-2 s-1
tendency_of_atmosphere_mass_content_of_seasalt_dry_aerosol_due_to_emission	emi_ss	kg m-2 s-1
tendency_of_atmosphere_mass_content_of_dust_dry_aerosol_due_to_emission	emi_du	kg m-2 s-1
tendency_of_atmosphere_mass_content_of_dimethyl_sulfide_due_to_emission	emi_dms	kg m-2 s-1
atmosphere_emission_mass_flux_of_anthropogenic_nox_as_nitrogen	emi_anox	kg m-2 s-1
atmosphere_emission_mass_flux_of_anthropogenic_carbon_monoxide	emi_aco	kg m-2 s-1
atmosphere_emission_mass_flux_of_anthropogenic_non_methane_volatile_organic_compounds_as_carbon	emi_avoc	kg m-2 s-1
atmosphere_emission_mass_flux_of_anthropogenic_ammonia	emi_anh3	kg m-2 s-1
atmosphere_emission_mass_flux_of_anthropogenic_sulfur_dioxide	emi_aso2	kg m-2 s-1
atmosphere_emission_mass_flux_of_anthropogenic_sulfate_as_sulfate_dry_aerosol	emi_aso4	kg m-2 s-1
atmosphere_emission_mass_flux_of_anthropogenic_black_carbon_dry_aerosol	emi_abc	kg m-2 s-1
atmosphere_emission_mass_flux_of_anthropogenic_particulate_organic_matter_as_particulate_organic_matter_dry_aerosol	emi_apom	kg m-2 s-1
atmosphere_emission_mass_flux_of_anthropogenic_secondary_organic_matter_as_secondary_organic_matter_dry_aerosol	emi_asoa	kg m-2 s-1
monthly mean radiative fluxes and forcings		
toa_outgoing_shortwave_flux	rsut	W m-2
toa_outgoing_longwave_flux	rlut	W m-2
toa_outgoing_longwave_flux_ assuming_clear_sky	rlutcs	W m-2
toa_outgoing_shortwave_flux_ assuming_clear_sky	rsutcs	W m-2
toa_net_downward_shortwave_flux	swtoaas_aer	W m-2
toa_net_downward_shortwave_flux	swtoacs_aer	W m-2

toa_net_downward_longwave_flux	lwtoaas_aer	W m-2
toa_net_downward_longwave_flux	lwtoacs_aer	W m-2
surface_downwelling_shortwave_flux_in_air	rsds	W m-2
surface_upwelling_shortwave_flux_in_air	rsus	W m-2
surface_downwelling_longwave_flux_in_air	rlds	W m-2
surface_upwelling_longwave_flux_in_air	rlus	W m-2
toa_net_downward_shortwave_flux_ozone	swtoaas_o3	W m-2
toa_net_downward_longwave_flux_ozone	lwtoaas_o3	W m-2
tropopause_net_downward_longwave_flux_ozone	lwtropas_o3	W m-2
tropopause_net_downward_shortwave_flux_ozone	swtropas_o3	W m-2
toa_net_downward_shortwave_flux_methane	swtoaas_ch4	W m-2
toa_net_downward_longwave_flux_methane	lwtoaas_ch4	W m-2
toa_net_downward_shortwave_flux_nitrous_oxide	swtoaas_n2o	W m-2
toa_net_downward_longwave_flux_nitrous_oxide	lwtoaas_n2o	W m-2
toa_net_downward_shortwave_flux_halocarbons	swtoaas_hc	W m-2
toa_net_downward_longwave_flux_halocarbons	lwtoaas_hc	W m-2
toa_net_downward_shortwave_flux_all_sky_SO4	swtoaas_so4	W m-2
toa_net_downward_shortwave_flux_all_sky_bcff	swtoaas_bcff	W m-2
toa_net_downward_shortwave_flux_all_sky_pomff	swtoaas_pomff	W m-2
toa_net_downward_shortwave_flux_all_sky_bb	swtoaas_bb	W m-2
toa_net_downward_shortwave_flux_clear_sky_bcff	swtoacs_bcff	W m-2
toa_net_downward_shortwave_flux_clear_sky_pomff	swtoacs_pomff	W m-2
toa_net_downward_shortwave_flux_clear_sky_bb	swtoacs_bb	W m-2
toa_net_downward_shortwave_flux_all_sky_soa	swtoaas_soa	W m-2
toa_net_downward_shortwave_flux_all_sky_no3	swtoaas_no3	W m-2
toa_net_downward_shortwave_flux_all_sky_ss	swtoaas_ss	W m-2
toa_net_downward_shortwave_flux_all_sky_dust	swtoaas_dust	W m-2
toa_net_downward_shortwave_flux_clear_sky_dust	swtoacs_dust	W m-2
toa_net_downward_longwave_flux_all_sky_dust	lwtoaas_dust	W m-2
atmosphere_optical_thickness_due_to_aerosol	od550_aer	1 (i.e., dim-less)

atmosphere_optical_thickness_due_to_aerosol	od440_aer	1 (i.e., dim-less)
atmosphere_optical_thickness_due_to_aerosol	od870_aer	1 (i.e., dim-less)
atmosphere_optical_thickness_due_to_pm1_ambient_aerosol	od550lt1_aer	1 (i.e., dim-less)
atmosphere_absorption_optical_thickness_due_to_aerosol	abs550_aer	1 (i.e., dim-less)
aerosol_asymmetry_parameter	asy_aer	1 (i.e., dim-less)
atmosphere_optical_thickness_due_to_sulfate_ambient_aerosol	od550_so4	1 (i.e., dim-less)
atmosphere_optical_thickness_due_to_black_carbon_ambient_aerosol	od550_bc	1 (i.e., dim-less)
atmosphere_optical_thickness_due_to_particulate_organic_matter_ambient_aerosol	od550_pom	1 (i.e., dim-less)
atmosphere_optical_thickness_due_to_secondary_particulate_organic_matter_ambient_aerosol	od550_soa	1 (i.e., dim-less)
atmosphere_optical_thickness_due_to_biomass_burning_ambient_aerosol	od550_bb	1 (i.e., dim-less)
atmosphere_optical_thickness_due_to_nitrate_ambient_aerosol	od550_no3	1 (i.e., dim-less)
atmosphere_optical_thickness_due_to_seasalt_ambient_aerosol	od550_ss	1 (i.e., dim-less)
atmosphere_optical_thickness_due_to_dust_ambient_aerosol	od550_dust	1 (i.e., dim-less)
atmosphere_optical_thickness_due_to_water_in_ambient_aerosol	od550_aerh2o	1 (i.e., dim-less)
aerosol_growth_factor_at_90_percent_relative_humidity	gf90_aer	1
aerosol_angstrom_exponent	ang4487_aer	1 (i.e., dim-less)
aerosol_angstrom_exponent	ang4467_aer	1 (i.e., dim-less)
aerosol_angstrom_exponent	ang5087_aer	1 (i.e., dim-less)
cloud_area_fraction	clt	1 (i.e., dim-less)
diagnostics for aerosol indirect effects		
cloud_droplet_effective_radius_at_liquid_water_cloud_top	cdr	m
cloud_droplet_number_concentration_in_liquid_water_clouds	cdnc	m-3
liquid_water_cloud_area_fraction	lcc	1 (i.e., dim-less)
atmosphere_cloud_liquid_water_content	lwp	kg m-2
planetary_albedo	albs	1 (i.e., dim-less)
air_temperature_at_cloud_top	ttop	K
potential_temperature_difference_between_700hPa_and_1000hPa	lts	K
atmosphere_cloud_ice_content	iwp	kg m-2
ice_cloud_area_fraction	icc	1 (i.e., dim-less)
cloud_crystal_effective_radius_at_ice_cloud_top	icr	m
atmosphere_optical_thickness_due_to_cloud	cod	1 (i.e., dim-less)
condensation_nuclei_number_concentration_at_liquid_water_cloud_top	ccn	m-3
stratospheric diagnostics		
zonal_mean_methane	zm_ch4	mole mole-1
zonal_mean_Cly	zm_cly	mole mole-1
zonal_mean_water	zm_h2o	mole mole-1
zonal_mean_HCl	zm_hcl	mole mole-1
zonal_mean_o3	zm_o3	mole mole-1
zonal_mean_age_of_air	zm_age	s
zonal_mean_temperature	zm_t	K
zonal_mean_zonal_wind	zm_u	m s-1
total_ozone_column	o3_col	kg m-2
miscellaneous		
lightning _flash_rate	flash_rate	flashes/km2/s

Table S1. Monthly output naming convention and units for ACCMIP simulations.

Table S2.1. CO emissions totals (Tg CO a-1)

Model	acchist			accrcp26		accrcp45		accrcp60		accrcp85	
	1850	1980	2000	2030	2100	2030	2100	2030	2100	2030	2100
CESM-CAM-superfast	564	1,148	1,248	1,105	790	***	***	1,206	966	1,189	873
CICERO	565	1,147	1,248	1,113	750	1,236	689	***	***	1,197	907
CMAM	823	1,375	1,502	***	***	1,424	906	***	***	1,436	1,116
EMAC	497	1,080	1,180	***	***	1,108	589	***	***	***	802
GEOSCCM	527	1,117	1,231	***	***	***	***	***	***	***	***
GFDL-AM3	568	1,146	1,246	1,104	786	1,174	655	1,204	961	1,188	868
GISS-E2-R	387	971	1,070	924	621	989	495	1,029	802	1,005	702
GISS-E2-TOMAS	***	***	***	***	***	***	***	***	***	***	***
HadGEM2	922	1,483	1,610	***	1,143	***	1,011	***	***	***	1,224
LMDzORINCA	407	991	1,093	944	640	***	***	1,049	821	1,025	722
MIROC-CHEM	384	962	1,064	922	605	***	***	1,024	790	1,006	688
MOCAGE	486	1,068	1,168	1,026	708	***	***	1,126	883	1,110	791
NCAR-CAM3.5	565	1,148	1,248	1,105	787	1,175	656	1,206	962	1,189	870
STOC-HadAM3	492	1,082	1,184	1,040	717	***	***	***	***	1,125	801
UM-CAM	480	1,047	1,148	1,011	700	1,077	570	***	***	1,093	781
MEAN	547	1,126	1,231	1,029	750	1,169	696	1,120	884	1,142	857
STD DEV	153	145	153	78	146	138	175	86	80	123	156

Table S2.2. NMVOC emission totals (Tg C a-1)

Model	acchist			accrcp26		accrcp45		accrcp60		accrcp85	
	1850	1980	2000	2030	2100	2030	2100	2030	2100	2030	2100
CESM-CAM-superfast	429	429	429	429	429	***	***	429	429	429	429
CICERO	411	462	461	462	438	462	438	***	***	462	435
CMAM	***	***	***	***	***	***	***	***	***	***	***
EMAC	450	560	580	***	***	597	586	***	***	***	682
GEOSCCM	495	578	627	***	***	***	***	***	***	***	***
GFDL-AM3	762	828	830	824	788	830	800	832	808	836	814
GISS-E2-R	721	807	830	851	834	869	885	865	922	876	988
GISS-E2-TOMAS	***	***	***	***	***	***	***	***	***	***	***
HadGEM2	69	96	106	***	83	***	78	***	***	***	82
LMDzORINCA	565	662	666	654	600	***	***	662	628	671	639
MIROC-CHEM	728	821	833	826	774	***	***	836	808	842	805
MOCAGE	942	1,049	1,059	1,050	990	***	***	1,061	1,024	1,069	1,030
NCAR-CAM3.5	578	665	668	662	616	671	633	673	643	679	651
STOC-HadAM3	573	697	722	771	710	***	***	***	***	794	904
UM-CAM	429	523	535	528	475	532	486	***	***	546	513
MEAN	550	629	642	706	612	660	558	765	752	720	664
STD DEV	232	254	255	196	249	167	288	200	201	202	284

Table S2.3. NOx emission totals (Tg N a-1), lightning NOx included.

Model	acchist			accrcp26		accrcp45		accrcp60		accrcp85	
	1850	1980	2000	2030	2100	2030	2100	2030	2100	2030	2100
CESM-CAM-superfast	12.1	44.3	50	34.3	23.6	***	***	39.5	23.2	48	31.7
CICERO	18.4	45.4	50.3	43.4	28.9	46.5	28.6	***	***	52.9	35.6
CMAM	18.3	44.1	50.8	***	***	37.2	20	***	***	43.6	27.3
EMAC	14.3	41.7	47.6	***	***	43.9	27.8	***	***	***	37
GEOSCCM	17.3	41.5	45	***	***	***	***	***	***	***	***
GFDL-AM3	13.8	40.9	46.2	39.7	24.5	43	27	41.2	25.1	49.8	35.8
GISS-E2-R	15.8	43.2	48.6	42.4	27.9	45.3	29.7	43.9	28.5	51.6	39.1
GISS-E2-TOMAS	***	***	***	***	***	***	***	***	***	***	***
HadGEM2	11.9	39.3	44.8	***	23.4	***	25.7	***	***	***	34.5
LMDzORINCA	***	***	***	***	***	***	***	***	***	***	***
MIROC-CHEM	23.9	51.6	57.3	51.8	36.7	***	***	53.8	39.2	62.4	53.4
MOCAGE	14.8	42.5	47.9	41.3	26	***	***	42.8	24.8	51.2	36.9
NCAR-CAM3.5	12.1	44.9	50.7	35.7	23.7	39	26	40.9	24.3	49.3	35.3
STOC-HadAM3	18.2	46	51.6	44.9	29.5	***	***	***	***	55.2	40.9
UM-CAM	17.4	43.8	49.2	44.1	29.2	47.3	31.5	***	***	53.7	40.7
MEAN	16	44	49.2	42	27.3	41.9	27	43.7	27.5	51.8	37.4
STD DEV	3.4	3	3.3	5.2	4.1	4	3.4	5.2	6	5	6.3

Table S2.4. Lightning NOx emission totals (Tg N a-1), from those models reporting separate numbers

Model	acchist			accrcp26		accrcp45		accrcp60		accrcp85	
	1850	1980	2000	2030	2100	2030	2100	2030	2100	2030	2100
CESM-CAM-superfast	3.8	4	4.2	3.9	3.9	***	***	4.1	4.7	4.5	5.4
CICERO	5	5	5	5	5	5	5	***	***	5	5
CMAM	4.5	4	3.8	***	***	3.3	2.8	***	***	3.1	2.1
EMAC	5.4	5.2	5.7	***	***	5.4	5.7	***	***	***	6.2
GEOSCCM	5	5	5	***	***	***	***	***	***	***	***
GFDL-AM3	4.5	4.4	4.4	4.7	4.9	4.7	5.4	4.6	5.5	4.8	6.1
GISS-E2-R	7.5	7.6	7.7	8	8	8.1	8.7	8	8.9	8.1	9.7
GISS-E2-TOMAS	***	***	***	***	***	***	***	***	***	***	***
HadGEM2	1.3	1.2	1.3	***	1.6	***	1.7	***	***	***	2.3
LMDzORINCA	***	***	***	***	***	***	***	***	***	***	***
MIROC-CHEM	9.3	9.5	9.7	10.2	10.4	***	***	10.4	11.5	10.5	13.3
MOCAGE	5	5.1	5.2	5.4	5.5	***	***	5.3	5.9	5.3	6.3
NCAR-CAM3.5	3.8	4	4.1	4.2	4.2	4.2	4.4	4.3	4.8	4.3	5.5
STOC-HadAM3	7	6.9	7.2	7.5	7.6	***	***	***	***	7.6	8.9
UM-CAM	5	5	5.2	5.6	5.6	5.6	6.1	***	***	5.6	7.5
MEAN	5.2	5.1	5.3	6.1	5.7	5.2	5	6.1	6.9	5.9	6.5
STD DEV	2	2	2.1	2.1	2.5	1.5	2.1	2.5	2.7	2.2	3.1

Table S2.1-4. Globally- and annually-averaged emissions for each model. Missing or not-applicable data are identified by ***. The multi-model mean and standard deviation are also documented

.